The alternative sigma factor σ^B plays a crucial role in adaptive strategies of *Clostridium difficile* during gut infection

Nicolas Kint[1,2], Claire Janoir[3], Marc Monot[1,2], Sandra Hoys[3], Olga Soutourina[1,2#], Bruno Dupuy[1,2], and Isabelle Martin-Verstraete[1,2]*

[1] Laboratoire Pathogénese des Bactéries Anaérobies, Institut Pasteur, Paris, France;
[2] University Paris Diderot, Sorbonne Paris Cité, Paris, France.
[3] EA 4043, Unité Bactéries Pathogènes et santé (UBaPS), Univ. Paris-Sud, Université Paris-Saclay, 92290 Châtenay-Malabry, France

[#] Present address: Institute for Integrative Biology of the Cell, CEA, CNRS, Univ. Paris-sud, F-91198 Gif sur Yvette cedex, France.

***Corresponding authors:** Laboratoire Pathogénese des Bactéries Anaérobies, Institut Pasteur, and University Paris Diderot, Sorbonne Paris Cité, Paris, France; *Phone*: +33140613561; *email:* isabelle.martin-verstraete@pasteur.fr

Key words: General stress response, ROS, nitric oxide, oxygen tolerance, acid stress, gut colonization, regulation

Role of σ^B in stress adaptation in *C. difficile*

This article has been accepted for publication and undergone full peer review but has not been through the copyediting, typesetting, pagination and proofreading process which may lead to differences between this version and the Version of Record. Please cite this article as an 'Accepted Article', doi: 10.1111/1462-2920.13696

Abstract

Clostridium difficile is a major cause of diarrhoea associated with antibiotherapy. Exposed to stresses in the gut, *C. difficile* can survive by inducing protection, detoxification, and repair systems. In several firmicutes, most of these systems are controlled by the general stress response involving σ^B. In this work, we studied the role of σ^B in the physiopathology of *C. difficile*. We showed that the survival of the *sigB* mutant during the stationary phase was reduced. Using a transcriptome analysis, we showed that σ^B controls the expression of ~25% of genes including genes involved in sporulation, metabolism, cell surface biogenesis, and the management of stresses. By contrast, σ^B does not control toxin gene expression. In agreement with the up-regulation of sporulation genes, the sporulation efficiency is higher in the *sigB* mutant than in the wild-type strain. *sigB* inactivation also led to increased sensitivity to acidification, cationic antimicrobial peptides, nitric oxide and ROS. In addition, we showed for the first time that σ^B also plays a crucial role in oxygen tolerance in this strict anaerobe. Finally, we demonstrated that the fitness of colonisation by the *sigB* mutant is greatly affected in a dixenic mouse model of colonisation when compared to the wild-type strain.

Introduction

Clostridium difficile is a gram-positive, anaerobic, spore-forming bacterium, found in soil, aquatic environments, and the mammalian intestinal tract. This enteropathogen is a major cause of antibiotic-associated diarrhoea and of pseudomembranous colitis, a potentially lethal disease. The incidence and severity of *C. difficile* infection (CDI) have increased in the early 2000s in North America and Europe owing to the emergence of new isolates belonging to the BI/NAP1/027 lineage (Rupnik et al., 2009; Wiegand et al., 2012). *C. difficile* is acquired from the environment through ingestion of spores: a form of transmission, resistance, and dissemination of this bacterium (Deakin et al., 2012). Disruption of the normal intestinal microbiota induces substantial changes in metabolite pools (Theriot et al., 2014) allowing for germination of the spores in the presence of a cholate conjugate and thereafter colonisation of the intestinal tract by the vegetative cells of *C. difficile.* Next, toxigenic strains of *C. difficile* produce two toxins, TcdA and TcdB, which are the major virulence factors. These toxins cause alteration of the actin cytoskeleton of intestinal epithelial cells and lead to major neutrophil recruitment favouring an intensive local inflammatory process (Peniche et al., 2013; Jose and Madan, 2016). Some *C. difficile* strains also produce an ADP-ribosylating binary toxin (Janoir, 2016). Although toxins are regarded as primary virulence factors, additional factors such as the adhesin Cwp66, the flagellum, the fibronectin-binding protein FbpA, and the surface layer protein SlpA participate in the colonisation process to enable the establishment of this bacterium in its colonic niche (Janoir, 2016). However, there is a lack of knowledge about additional virulence or colonisation factors as well as molecular mechanisms controlling their production in response to environmental signals detected in the gut or involved in adaptive strategies used by *C. difficile* during infection.

During all the steps of the infection cycle, *C. difficile* encounters several stresses. *C. difficile* spores have to face oxygen (O_2) present in the atmosphere, and after ingestion, are exposed to acidic pH of the stomach. After germination, vegetative cells encounter different stresses such as pH variations and hyperosmolarity and are exposed to bile acids, to antibiotics, or to cationic antimicrobial peptides (CAMPs) produced by the host and/or by the microbiota (Abt et al., 2016). Moreover, during infection, *C. difficile* produces several factors (e.g., toxins, S-layer proteins, and flagellin) that trigger inflammation leading to the production of several antimicrobial compounds by the host immune system, e.g., reactive oxygen species (ROS), nitric oxide (NO), and reactive nitrogen species (RNS) (Abt et al., 2016; Jose and Madan, 2016). Thus, to adapt to and survive the exposure to these stresses within the host, *C. difficile* must induce protection, detoxification, and repair pathways as well as regulatory networks sensing these stressful stimuli.

One of the most effective responses to a wide range of stresses and starvation conditions in several firmicutes is the general stress response involving the alternative sigma factor, σ^B (Hecker et al., 2007). Indeed, depending on the bacterial species, a mutant with inactive σ^B is more sensitive to acidic or alkaline pH, high osmolarity, ethanol, some antibiotics, bile acids, oxidative stress, or temperature variations (Ferreira et al., 2001; Giachino et al., 2001; Bandow et al., 2002; Zhang et al., 2011; Reder et al., 2012b). As a sigma factor, σ^B is a sequence-specific DNA-binding subunit of RNA polymerase that ensures the recognition of appropriate promoters upstream of the controlled genes and their transcription. The σ^B regulon has been identified in *Bacillus subtilis*, *Bacillus cereus*, *Staphylococcus aureus*, and *Listeria monocytogenes* (Price et al., 2001; Bischoff et al., 2004; van Schaik et al., 2007; Nannapaneni et al., 2012; Mader et al., 2016). σ^B positively controls the expression of 100 to 200 genes (Guldimann et al., 2016). Some σ^B-controlled genes are directly related to stress resistance, whereas others are involved in different cellular functions such as metabolism, cell envelope homeostasis, biofilm formation, and virulence (Guldimann et al., 2016). Expression of the σ^B regulon confers onto the bacterium global protection from adverse conditions; however, it represents a major cost for the bacteria. Therefore, σ^B activity has to be tightly controlled with rapid and strong induction upon stress exposure or during the stationary growth phase and by silencing in the exponential growth phase. σ^B activity is controlled by a well-conserved post-translational mechanism, called partner switching, in which interaction and activation of proteins are driven by reversible threonine and serine phosphorylation (Yang et al., 1996; Hecker et al., 2007). In unstressed cells and during the exponential growth phase, the anti-σ factor and kinase RsbW phosphorylates the anti-anti-σ factor RsbV and sequesters σ^B thereby preventing its association with the core enzyme of RNA polymerase. When cells are exposed to a stress or in the stationary phase, a signal is transmitted to specific PP2C phosphatase(s) that dephosphorylate(s) RsbV, allowing this anti-anti-σ factor to interact with RsbW, thus leading to the release and activation of σ^B. The phosphorylated state of RsbV is the key element of σ^B activation or silencing. Signals triggering phosphatase activation that leads to a σ^B release depend on the bacterial species (de Been et al., 2011). Indeed, osmolytes, heat, and ethanol commonly stimulate phosphatase activity in many firmicutes, whereas low pH is a trigger signal valid only in *B. subtilis* and *L. monocytogenes* (de Been et al., 2011; Guldimann et al., 2016). In *B. subtilis*, another σ^B-activating pathway mediated by the PP2C phosphatase, RsbP, is dependent on the energetic state of the bacterium (Vijay et al., 2000; Hecker et al., 2007).

The three genes *rsbV*, *rsbW*, and *sigB*-encoding proteins involved in the partner switching mechanism activating the general stress response are present only in the genome of a few clostridia including *Clostridium thermocellum*, *C. cellulotycum*, *C. sticklandii*, and the two pathogens *C. sordellii* and *C. difficile*. However, the general stress response has never been studied in clostridia. In the present work, we studied the role of σ^B in the physiology and stress response in *C. difficile.* Using a transcriptomic analysis, we showed that σ^B plays a pleiotropic role in *C. difficile* by controlling genes involved in metabolism, sporulation, and stress responses. Accordingly, we found that a *sigB* mutant is more sensitive to various stresses mimicking those *C. difficile* encounters during its infectious cycle, particularly the oxidative/nitrosative stress, and its colonisation fitness is highly affected in the gut of a dixenic mouse model of colonisation.

Results and discussion

Growth stage-dependent phenotypes of the *C. difficile sigB* mutant.

In *B. subtilis*, *B. cereus*, *L. monocytogenes*, and *S. aureus*, the *sigB* gene belongs to an operon with *rsbV* and *rsbW* encoding the anti-anti-σ factor and the anti-σ factor of σ^B, respectively (Hecker et al., 2007). In *C. difficile*, the *sigB* gene (*CD0011*) is the last gene of a locus containing five genes. *CD0007* and *CD0008* encode two small proteins of unknown function. CD0009 and CD0010 share 35% and 39% identity with RsbV and RsbW of *B. subtilis*, respectively. To identify the role of σ^B in the *C. difficile* physiology, we constructed a *sigB* mutant in the strain 630Δ*erm* using the ClosTron system. A group II intron was inserted into the *sigB* gene in sense orientation immediately after the 33rd nucleotide in its coding sequence (Fig S1A). We observed similar growth of the 630Δ*erm* strain and of the *sigB* mutant in both tryptone-yeast extract (TY) and brain heart infusion (BHI) media (Fig 1A and S2A). This result indicates that σ^B is not essential for *C. difficile* growth in a rich medium, in agreement with the data from other firmicutes (Hecker et al., 2007; Guldimann et al., 2016). Because σ^B is a stationary-phase σ factor (Hecker et al., 2007), we tested the survival rate of strain 630Δ*erm* and of the *sigB* mutant at 24, 48, and 72 h of growth in TY, a medium that does not favour the sporulation process. After 48 h of growth, the survival rate was five-fold higher for the 630Δ*erm* strain (31%) than for the *sigB* mutant (6.5%), and the difference increased to 15-fold at 72 h (Fig 1B). These results revealed that σ^B participates in the survival of *C. difficile* during the stationary phase as observed for *L. monocytogenes* (Bruno and Freitag, 2011).

We wondered whether σ^B is involved in the ability of *C. difficile* to form a biofilm as observed in *B. subtilis*, *S. aureus*, and *L. monocytogenes* (van der Veen and Abee, 2010; Guldimann et al., 2016). Because the R20291 strain, which belongs to the BI/NAP/027 family, is known to form a more robust biofilm than the 630Δ*erm* strain does (Ethapa et al., 2013), we also constructed a *sigB* mutant from the R20291 strain (Fig S1C). No significant difference in the magnitude of biofilm formation was observed between the wild-type and the *sigB* mutant strains in both backgrounds under the conditions used (Fig S2B) suggesting that σ^B is not involved in the control of biofilm formation in *C. difficile*.

Comparative analysis of gene expression profiles of 630Δ*erm* and the *sigB* mutant strains at the onset of the stationary phase.

To identify genes regulated by σ^B, we compared the expression profiles of the 630Δ*erm* strain and of the *sigB* mutant at the onset of the stationary phase (10 h). Approximately 25% of the *C. difficile* genes were differentially expressed between these two strains. 595 genes and 410 genes were up- and down-regulated in the *sigB* mutant. No difference in expression was detected for the *CD0007*, *CD0008*, *rsbV* and *rsbW* genes between the *sigB* mutant and the wild-type strain. Of note, ~20% of the genes induced at the onset of the stationary phase (Saujet et al., 2011) are positively controlled by σ^B. σ^B regulates numerous genes involved in carbon, amino acid, sulphur, base, and co-factor metabolism, motility, sporulation, cell-wall metabolism, and stress responses (Table 1 and Table S1 to S5). It is noteworthy that ~10% of the genes controlled by σ^B have an unknown function, as in other firmicutes (Bischoff et al., 2004; Hecker et al., 2007). Some of these genes may be involved in stress management in *C. difficile*. Moreover, we found that *tcdA* and *tcdB* encoding *C. difficile* toxins were not differentially expressed according to both transcriptomic and qRT-PCR experiments. Using ELISAs, we confirmed that toxin production was similar in the 630Δ*erm* strain and in the *sigB* mutant (Fig S2C). Thus, contrary to TcdR (Mani and Dupuy, 2001), σ^D (El Meouche et al., 2013), σ^H (Saujet et al., 2011), and σ^L (Dubois et al., 2016), σ^B does not control toxin production in *C. difficile.*

To validate the transcriptomic data, qRT-PCR were performed on a subset of ~50 genes involved in various biological processes (Table S1). The qRT-PCR results confirmed the transcriptomic data for all the tested genes. To demonstrate that the differential expression observed in the transcriptome was due to the absence of σ^B, we complemented the *sigB* mutant. For this purpose, the *sigB* gene was cloned into pRPF185 with the promoter region, called P_{sigB}, located upstream of *CD0007*. The transfer of the resulting plasmid (pDIA6325) into the *sigB* mutant led to *sigB* gene overexpression (~10-fold). We showed that the expression of several genes was fully or at least partially restored in the complemented strain when compared to the 630Δ*erm* strain (Table S1).

In conclusion, σ^B plays a pleiotropic role in the control of transcription in *C. difficile* as observed in *Bacillus*, *Staphylococcus*, and *Listeria* species (Bischoff et al., 2004; Nannapaneni et al., 2012; Guldimann et al., 2016; Mader et al., 2016). However, the size of the σ^B regulon is larger in *C. difficile* than in these firmicutes.

Negative control of sporulation by σ^B.

We found that more than 200 genes encoding proteins involved in all steps of spore formation or transcribed under the control of the four sporulation-specific σ factors (Lawley et al., 2009; Fimlaid et al., 2013; Saujet et al., 2013) were differentially expressed in the *sigB* mutant compared to the 630Δ*erm* strain (Table S2). Remarkably, most genes of the σ^F, σ^E, and σ^G regulons (84%, 96%, and 96%, respectively) were up-regulated in the *sigB* mutant. By contrast, only 38% of the σ^K regulon was derepressed in the *sigB* mutant under the conditions tested. The timing of cell sampling (10 h) is probably too early to detect full induction of σ^K targets involved in the late stages of sporulation (Fimlaid et al., 2013; Saujet et al., 2013; Pishdadian et al., 2015). To confirm the control of sporulation by σ^B, we compared the sporulation efficiency of the *sigB* mutant and 630Δ*erm* strain after 72 h of growth in the sporulation medium. In line with the transcriptomic data, the *sigB* mutant produced ~10-fold more spores (3.3×10^6 spores·ml^{-1}) than the 630Δ*erm* strain did (2.5×10^5 spores·ml^{-1}). The sporulation rate was ~7% for the 630Δ*erm* strain and ~37% for the *sigB* mutant. Finally, spore germination was compared. After the addition of taurocholate and glycine, OD_{600nm} of the treated spores dropped rapidly in both strains because of Ca^{2+}-dipicolinic acid release and reached a plateau at a value corresponding to ~65% of the initial OD_{600nm} after 30 min of incubation (Fig S2D). All these results indicate that σ^B negatively controls sporulation but does not affect germination.

Key sporulation genes expressed in pre-divisional cells such as *spoIIAA-spoIIAB-sigF*, *spoIIE*, and *spoIIAG-sigE*, or after asymmetric division, e.g. members of the σ^F and σ^E regulons (Saujet et al., 2013), were strongly repressed by σ^B, suggesting that σ^B acts at the initiation of sporulation. Moreover, σ^B controls in *B. subtilis* the expression of *spo0E*, which encodes one of the Spo0A phosphatases and overexpression of *sigB* decreases sporulation efficiency (Reder et al., 2012c; Reder et al., 2012a). In our transcriptomic data, the expression of *CD1579* encoding a histidine kinase that phosphorylates Spo0A *in vitro* (Underwood et al., 2009) was up-regulated in the *sigB* mutant. No phosphatase of Spo0A-P has been identified in *C. difficile* to date, but in *Clostridium acetobutylicum*, one kinase (Cac0437) has lost the ability to auto-phosphorylate and catalyses the ATP-dependent dephosphorylation of Spo0A-P (Steiner et al., 2011). Interestingly, *CD1492,* encoding a kinase sharing 30% identity with Cac0437, was down-regulated in the *sigB* mutant. Furthermore, it was recently reported that CD1492 negatively controls sporulation (Childress et al., 2016). In conclusion, we propose that σ^B controls sporulation initiation by modulating the level of phosphorylation of Spo0A as suggested in *B. subtilis*.

Involvement of σ^B in cell envelope homeostasis.

By forming a physical barrier between the cell and the environment, the cell wall and cell membrane play a crucial role in stress protection and in transmission of stress signals. We deduced from our transcriptome analysis that σ^B controls the expression of several genes encoding membrane- and cell wall-associated proteins as well as proteins involved in cell wall metabolism (Table S3 and S4).

Some genes involved in motility are differentially expressed between the wild-type and mutant strains (Table S3). Indeed, several genes belonging to one of the two large flagellar operons were down-regulated in the *sigB* mutant. However, we did not detect a defect in motility in the *sigB* mutant compared to strain 630Δ*erm* under our conditions (0.3% BHI agar plates), suggesting that the decrease in the expression of these genes is not sufficient to inhibit motility. Several genes involved in the formation of type IV pili (T4P) were also differentially expressed in the *sigB* mutant compared to the wild type strain. *C. difficile* possesses a complete primary T4P operon and a secondary gene cluster, which encode a single pilin (*pilA2-CD3294*) and T4P assembly components (*pilB2-CD3296*, *pilC2-CD3295*, and *pilM2-CD3293*). The expression of the genes belonging to the secondary T4P cluster (*CD3293-96*) and of *pilD2* (*CD3503*) that encodes a pre-pilin peptidase was up-regulated in the *sigB* mutant (Table S3). By contrast, the gene *CD3513* encoding the major pilin (PilA1) in this primary cluster was down-regulated in the *sigB* mutant. Because T4P are involved in surface motility (Purcell et al., 2016), we tested the ability of the wild-type strain and *sigB* mutant in the 630Δ*erm* and R20291 backgrounds to migrate across the surface of BHI plates in the presence of an increasing agar concentration (1% to 2%). We did not see a significant difference in surface behaviour between the wild-type strain and mutant strain under these conditions. The role of the second T4P cluster has never been determined, and its strong repression by σ^B is the first evidence of regulation for these genes.

Our transcriptomic data also showed that the expression of several genes encoding surface-associated proteins (Janoir, 2016) decreased in the *sigB* mutant (Table S3). This set includes genes encoding the S-layer precursor (*slpA*), putative autolysins (*CD2767-cwp19* and *CD2784-cwp6*), a collagen-binding protein (*cbpA*), two adhesins (*CD2831* and *CD3246*) anchored to peptidoglycan by a sortase (Peltier et al., 2015), and other cell wall-associated proteins of unknown function such as CD0440 (Cwp27), CD2518 (Cwp29), and CD2791 (Cwp2). This situation is reminiscent of the positive control by σ^B of cell wall adhesins and a fibronectin-binding protein in *S. aureus* (Entenza et al., 2005; Mitchell et al., 2008) and of the internalin InlA, of LPXTG-containing proteins anchored by sortase A, and potential collagen-binding proteins in *L. monocytogenes* (Oliver et al., 2009; Quereda et al., 2013). By contrast, genes encoding the lipoprotein CD0873 involved in adhesion of *C. difficile* to Caco-2 cells (Janoir, 2016), the fibronectin-binding protein FbpA, and a cell wall-binding protein of unknown function (*cwp28/CD1987*) were up-regulated in the *sigB* mutant. These results strongly suggested that σ^B largely controls the composition of surface-associated proteins in *C. difficile*.

Finally, σ^B controls *C. difficile* genes encoding proteins involved in cell wall metabolism. Several genes implicated in peptidoglycan synthesis including genes involved in the production of the disaccharide-pentapeptide associated with a lipid carrier (*murA*, *murC*, *murD*, *murE*, *murF*, *mraY*, *murG, uppS*, and *uppP1* genes) or encoding a probable peptidoglycan glycosyltransferase (*CD1229*), an L,D-trans-peptidase (*CD3007*), a glutamate racemase (*murI*), and an alanine racemase (*CD3463*) were more strongly expressed in the *sigB* mutant compared to the wild-type strain (Table S4). We also observed increased expression in the *sigB* mutant of genes encoding two putative N-acetyl-muramoyl-L-alanine amidases (CD0784 and CD2761), a putative lytic trans-glycosylase (CD1130), and a serine-type D-Ala-D-Ala carboxypeptidase (CD2141). By contrast, genes encoding a probable deacetylase of peptidoglycan (CD1522), another L,D-transpeptidase (CD2963), a D-Ala-D-Ala-carboxypeptidase (CD2504), or two cell-wall hydrolases (CD0183, CD1898) were less strongly expressed in the *sigB* mutant compared to the 630Δ*erm* strain (Table S4).

Several phenotypic assays associated to cell wall or to cell surface properties were performed. We did not see a difference in the sensitivity to lysozyme between the wild-type strain and *sigB* mutant while the *sigB* mutant is more sensitive than the wild-type strain to two CAMPs, bacitracin and polymyxin B. Indeed, the minimal inhibitory concentration (MIC) for bacitracin was 560 ± 85 μg·ml^{-1} for the 630Δ*erm* strain and 140 ± 25 μg·ml^{-1} for the *sigB* mutant, while the MIC for polymyxin B was 340 ± 27 μg·ml^{-1} for the wild-type strain and 180 ± 19 μg·ml^{-1} for the mutant. These data are consistent with the decreased expression in the *sigB* mutant of *dltA* and *dltD* involved in teichoic acid D-alanylation, a mechanism of protection from CAMPs in *C. difficile* (McBride and Sonenshein, 2011b). By contrast, σ^B does not control the expression of *cprABC* encoding an ABC transporter involved in removal of CAMPs (McBride and Sonenshein, 2011a). Because polymyxin B is known to increase ROS formation (Yu et al., 2015), the increased toxicity of polymyxin B for the *sigB* mutant may be due to the increased sensitivity of this mutant to ROS (see below). However, we cannot rule out that other genes involved in uncharacterised mechanisms of CAMPs resistance in *C. difficile* are controlled by σ^B. As observed in *L. monocytogenes* and *S. aureus* (Guldimann et al., 2016), σ^B seems to participate in the cell envelope homeostasis in *C. difficile*.

σ^B is a global regulator of central metabolism.

Many genes involved in central metabolism (Table S5) are controlled by σ^B. Several genes encoding proteins of the phosphoenolpyruvate-dependent sugar phosphotransferase system (PTS) are differentially expressed in the *sigB* mutant compared to the wild-type strain, as observed in *L. monocytogenes* (Guldimann et al., 2016). Genes encoding PTS specific for glucose, fructose, cellobiose, and β-glucoside (*CD2666-67*, *CD2269*, *CD3089*, and *CD3137-38*, respectively) and the *ptsH* gene encoding HPr, a general component of the PTS, were negatively controlled by σ^B (Fig S3) whereas gene encoding xylosides and galactitol PTS transporters allowing utilization of alternative carbon sources were positively controlled by σ^B Most of the genes involved in glycolysis were also more strongly expressed in the *sigB* mutant, while genes involved in glycogen biosynthesis were less strongly expressed in this mutant (Fig S3). Thus, all these results pointed to an increase in the import of glucose or glucose-containing compounds, a drop in carbon storage, and enhanced flux into glycolysis in the *sigB* mutant. In addition, differences in the expression of genes of fermentation pathways were observed. The *CD2966* gene (*adhE*) encoding an aldehyde-alcohol dehydrogenase participating in ethanol and butanol production is up-regulated in the *sigB* mutant while genes *CD0112-13* and *CD2379* encoding enzymes involved in butyrate production are down-regulated (Fig S3).

In addition, several genes encoding putative peptidases or proteases as well as genes encoding amino acid transporters were differentially expressed in the *sigB* mutant compared to in the wild-type strain (Fig S4 and Table S5). When the *sigB* gene was disrupted, the expression of genes involved in the biosynthesis of histidine and asparagine increased, while the expression of genes involved in the biosynthesis of aspartate and cysteine as well as in the catabolism of glutamate, glutamine, and leucine decreased. It is noteworthy that σ^B also positively controls the expression of genes of synthesis of several co-factors such as cobalamin, folate and molybdenum (Table S5). These co-factors are required for the metabolism of fatty acids, amino acids, carbon sources and nucleic-acids.

These results suggested that σ^B participates in extensive reprogramming of cellular metabolism at the onset of the stationary phase or in a stressful environment. It is worth noting that in *B. subtilis*, *S. aureus*, and in *L. monocytogenes*, a large number of genes positively controlled by σ^B are similarly involved in metabolism and mostly in energy metabolism as we observed in *C. difficile* (O'Byrne and Karatzas, 2008; Guldimann et al., 2016). This observation is suggestive of possible adaptation to metabolic pathways required for host colonisation. The *sigB* mutant of *L. monocytogenes* has a reduced ability to grow on glycerol, an alternative energy source during intracellular life of the bacteria (Guldimann et al., 2016).

The role of σ^B in the control of DNA repair and in resistance to antibiotics and bile salts.

σ^B plays a crucial role in the general stress response in several gram-positive bacteria via its control of genes encoding proteins that protect the cells from stress or that repair cellular damage (Hecker et al., 2007). However, such a function of σ^B has never been studied in anaerobic firmicutes. To determine the role of σ^B in the stress response in *C. difficile*, we decided to focus our study on stresses that *C. difficile* likely encounters in the host during infection and on stresses related to genes differentially expressed according to the transcriptome analysis. We also analysed genes identified by Emerson et al. (Emerson et al., 2008) as participants in the transcriptional response of *C. difficile* to several environmental and antibiotic stresses.

In *C. difficile*, ~55 genes that probably participate in stress management were controlled by σ^B. The expression of a few of them, such as those encoding the GroES and GroEL chaperones, a heat-shock protein (CD3219), or a multidrug family ABC-transporter (CD3198), increased in the *sigB* mutant compared to in the 630Δ*erm* strain (Table 1). In contrast, σ^B positively controls many genes involved in the response to stressful stimuli (Table 1). The expression of *uvrABC* as well as *mutS* decreased in the *sigB* mutant compared to the wild-type strain. The UvrABC and MutS proteins are involved in DNA repair suggesting that σ^B participates in the response to DNA damage. We therefore compared the sensitivity of the 630Δ*erm* strain and *sigB* mutant to several antibiotics known to induce DNA damage. The rates of sensitivity to ciprofloxacin, norfloxacin and metronidazole were similar between the *sigB* mutant and the parental strain. However, for mitomycin C, known to causes DNA alkylation, the diameter of the growth inhibition area for the *sigB* mutant increased by more than 50%, as compared to the 630Δ*erm* strain (Fig 2A). In *C. difficile*, UvrABC is a target of the SOS response regulator LexA (Walter et al., 2014). Therefore, we tested other antibiotics known to induce the SOS response such as rifampicin, trimethoprim or tetracycline. However, we found that the *sigB* mutant was more sensitive than the parental strain only when the cells were exposed to rifampicin (Fig 2B) as observed in *B. subtilis* (Bandow et al., 2002). These results and the presence of only four genes positively controlled by σ^B among the 37 predicted *C. difficile* LexA targets (Walter et al., 2014) indicated the absence of a direct link between the SOS response and σ^B. Since rifampicin induces in *B. subtilis* the activity of σ^B and members of the oxidative stress stimulon (Bandow et al., 2002), it is possible that the oxidative stress induced by this antibiotics is responsible for the higher sensitivity of the *sigB* mutant to this compound in *C. difficile* (see below). It is also known that disruption of the *mutS* gene leads to increased mutation rates (Oliver et al., 2002) conferring a selective advantage in stressful or fluctuating environments. However, we did not observe a significant difference in the rate of ciprofloxacin resistance-related acquired mutations between the wild-type strain and the *sigB* mutant, suggesting that the decrease in the expression of *mutS* in this mutant is not sufficient to confer a hypermutable phenotype.

In the course of gut infection, *C. difficile* copes with exposure to bile salts, which play a key role in *C. difficile* physiology. Indeed, the primary bile salt cholate and its conjugated forms promote germination of *C. difficile* spores, whereas the secondary bile salt deoxycholate is toxic to vegetative cells (Sorg and Sonenshein, 2008). In *L. monocytogenes*, σ^B participates in the protection from bile salts (O'Byrne and Karatzas, 2008). σ^B positively controls *opuCA* and *opuCC* in *C. difficile* (Table 1). OpuCA shares 48% and 53% similarity, respectively with BilE, a bile efflux system and OpuCA, an osmoprotectant solute transporter of *L. monocytogenes*. However, we failed to detect under our experimental conditions a difference in sensitivity between the 630Δ*erm* strain and the *sigB* mutant when they were exposed to bile extracts, deoxycholate and cholate, or to NaCl (Fig S5). This finding suggests that σ^B does not play a major role in the stress response to bile salts or in osmoprotection in *C. difficile*.

Involvement of σ^B in the response to acid stress.

Several studies showed that pH values vary along the intestinal tract and among individuals according to their health state (Nugent et al., 2001). In *L. monocytogenes* and *B. subtilis*, the management of acid stress involves σ^B (Cotter and Hill, 2003; Hecker et al., 2007; Mols and Abee, 2011). To test whether σ^B contributes to the response to low pH in *C. difficile*, we performed serial dilution plating assays using TY agar plates at different pH levels (Fig 3). No growth was observed at pH 4.5 in the parental strain, the *sigB* mutant, and the complemented strain, but they grew similarly at pH 7, 6.5, and 6 (Fig 3). By contrast, compared to the parental and complemented strains, the growth of the *sigB* mutant was slightly and severely affected at pH 5.5 and 5.0, respectively, indicating that σ^B controls, at least partly, the acid stress management. It is worth mentioning that the pH level can locally reach 5.5 in the proximal colon probably because of short-chain fatty-acid production (Nugent et al., 2001). In *L. monocytogenes* and *B. cereus*, glutamate decarboxylase and arginine deiminase activities, which allow for consumption of intracellular protons or the production of NH_4^+, participate in acidic resistance (Cotter and Hill, 2003; Mols and Abee, 2011). No orthologues of these genes are present in the *C. difficile* genome. However, the expression of *glsA* (*CD0558*) and *gluD* (*CD0179*) encoding a glutaminase and a NAD-specific glutamate dehydrogenase, respectively, was positively controlled by σ^B. GlsA converts glutamine into glutamate and NH_4^+, while GluD mediates the oxidative deamination of glutamate to produce α-ketoglutarate and NH_4^+ (Fig S4) (Girinathan et al., 2016). The down-regulation of *glsA* and *gluD* genes in the *sigB* mutant that probably leads to reduced production of NH_4^+ might contribute to the increased sensitivity of this mutant to lower pH. Furthermore, it is worth noting that genes encoding hydrogenases such as *CD0893* and *CD3313-15* (*hydN1-hydA-hydN2*; Fig S3) were down-regulated in the *sigB* mutant. Hydrogenases, which catalyse the reversible reduction of H^+ to H_2, enable elimination of an excess of reducing power and protons. Thus, the low expression of hydrogenase genes in the *sigB* mutant may increase proton concentration and acid sensitivity. Moreover, it is possible that substantial rerouting of metabolism leads to accumulation of compounds that contribute to increased sensitivity of the *sigB* mutant to acid stress. Finally, the cell envelopes also play a role in the acid resistance because mutation of genes involved in the biogenesis, assembly, or maintenance of the cell wall leads to higher sensitivity of the cell to acidic pH (Cotter and Hill, 2003). Thus, during the infection process, the ability of *C. difficile* vegetative cells to cope with pH variations along the intestinal tract might involve σ^B. However, the molecular mechanisms underlying the adaptation to acidic stress have yet to be elucidated.

The function of σ^B in the nitrosative-stress response.

In the course of infection, *C. difficile* produces two toxins TcdA and TcdB that alter the enterocyte cytoskeleton, thereby inducing intestinal-cell lysis and inflammation (Abt et al., 2016; Janoir, 2016). Indeed, the death of the epithelial cells triggers secretion of multiple factors stimulating major recruitment of neutrophils, which leads to an intensive local inflammatory reaction (Abt et al., 2016; Jose and Madan, 2016). During the inflammation process, ROS including hydrogen peroxide (H_2O_2) and O_2^- as well as NO and its derivative reactive species (RNS) are produced at bactericidal concentrations by the host immune cells. In our transcriptome data, we found that some genes encoding proteins potentially involved in NO and RNS detoxification, are positively controlled by σ^B (Table 1). Indeed, the expression of *CD1157* (*norV*) encoding a putative NO-reductase and of two genes (*CD1125* and *CD0837)* encoding nitro-reductases, decreased 20-, 17-, and two-fold, respectively, in the *sigB* mutant compared to the strain 630Δ*erm*. Moreover, the expression of *CD1822* (*hcp*), which encodes a hydroxylamine reductase that could be used for a NO detoxification process, also decreased five-fold in the *sigB* mutant (Table 1 and Table S1). To test the involvement of σ^B in the control of NO detoxification, we compared the sensitivity of 630Δ*erm*, the *sigB* mutant, and the complemented strain to sodium nitroprusside (SNP) and di-ethylamine NoNoate (DEA/NO), two NO donor compounds, by plating serial dilutions of these strains or by growth monitoring in a liquid medium. After 24 h of incubation on plates, the *sigB* mutant had a growth defect in the presence of DEA/NO or SNP as compared to the parental and complemented strains in both 630Δ*erm* and R20291 backgrounds (NAP/027) (Fig 4A and Fig S6A). Furthermore, in a liquid medium, the growth of the *sigB* mutant in the 630Δ*erm* background was reduced or abrogated in the presence of 5 and 10 µM of DEA/NO, respectively (Fig 4C and 4D) or in the presence of 10 and 20 µM of SNP (Fig S6C and S6D), respectively, while the growth of the wild-type and complemented strains was only slightly affected under these conditions compared to the TY medium (Fig 4B and Fig S6B). We next compared the survival among the parental strain, the *sigB* mutant, and the complemented strain after 30 min of exposure to SNP or DEA/NO. The survival was 40- and 13-fold higher in 630Δ*erm* than in the *sigB* mutant when exposed to 40 µM SNP and to 25 µM DEA/NO, respectively. Altogether, these results strongly suggested that σ^B performs an important function in the management of nitrosative stress that *C. difficile* has to face during the infectious cycle in the host.

In *S. aureus*, the members of the σ^B regulon are not induced after NO treatment suggesting that σ^B is not involved in the NO response (Hochgrafe et al., 2008). In *B. subtilis*, SNP or NO gas induces the expression of some σ^B-controlled genes (Moore et al., 2004; Rogstam et al., 2007) only under aerobic conditions. In contrast, a *sigB* mutant does not show increased sensitivity to SNP as compared to the wild-type strain (Rogstam et al., 2007). Thus, σ^B may be more crucial for the management of NO stress in *C. difficile* than in *B. subtilis*.

Involvement of σ^B in oxidative-stress management.

During inflammation, aside from NO and RNS, ROS are also produced by the host immune cells (Abt et al., 2016; Jose and Madan, 2016). Thus, we also wondered whether σ^B plays a role in the management of ROS. Using disk diffusion assays, we showed that the growth inhibition area for the *sigB* mutant increased in the presence of H_2O_2 (1 M) or paraquat (2 M, an O_2^- anion donor) from 30% to 60% as compared to the parental and complemented strains in the 630Δ*erm* and R20291 genetic backgrounds (Fig 5A and 5B, respectively). It thus appeared that inactivation of σ^B increased the sensitivity of *C. difficile* to ROS, indicating that σ^B is involved in the response to H_2O_2 and O_2^-. Strict anaerobes use original and specific reduction pathways for ROS detoxification leading to H_2O production rather than O_2 production as classically observed in other bacteria with catalase and superoxide dismutase (Lumppio et al., 2001; Hillmann et al., 2009b; Riebe et al., 2009). In *C. acetobutylicum*, as in other anaerobes, reverse rubrerythrin reducing H_2O_2 to H_2O by means of NADH as an electron donor, a desulfoferrodoxin acting like a superoxide reductase producing H_2O_2 from O_2^-, and a rubredoxin and a NADH:rubredoxin oxidoreductase (NROR) enable electron transfer from NAD(P)H to ROS (Riebe et al., 2009). Proteins sharing similarities with these enzymes involved in ROS detoxification are present in *C. difficile.* Of note, the expression of *CD0827*, encoding the desulfoferrodoxin of *CD1474* and *CD1524*, encoding reverse-rubrerythrins, and of *CD0176* and *CD1623*, encoding proteins similar to NADH-rubredoxin reductases, strongly decreased (5- to 100-fold) in the *sigB* mutant compared to the wild-type strain, according to the transcriptomic data and qRT-PCR experiments both in the 630Δ*erm* and the R20291 backgrounds (Table 1, S1 and S6). Although the role of these proteins in ROS detoxification remains to be experimentally characterised in *C. difficile*, it seems likely that the control of their transcription by σ^B contributes to the increased sensitivity of the *sigB* mutant to ROS exposure. In addition, the expression of *gluD*, encoding a glutamate dehydrogenase that is involved in *C. difficile* in H_2O_2 protection via an uncharacterised mechanism, also decreased three-fold in the *sigB* mutant (Girinathan et al., 2014).

It is worth noting that σ^B also participates in the oxidative-stress response in *B. subtilis*, *L. monocytogenes*, and *S. aureus*. Indeed, the viability of a *sigB* mutant of *L. monocytogenes* and *S. aureus* decreases when exposed to H_2O_2 or hydroperoxide donor compounds (Ferreira et al., 2001; Cebrian et al., 2009). Moreover, in *B. subtilis*, the *sigB* mutant is more sensitive to oxidative stress when cells are pre-adapted to a stress such as glucose starvation known to induce the activity of σ^B before exposure to H_2O_2 or paraquat (Engelmann and Hecker, 1996; Reder et al., 2012b). Thus, σ^B is required for implementation of protection from oxidative stress in most of the firmicutes containing this σ factor.

The control of tellurite resistance by σ^B.

We found in our transcriptome data that σ^B positively controls the expression of both the *CD1634-39* operon and *CD1652* gene, which are likely involved in the resistance to tellurite (K_2TeO_3), a compound known to generate ROS (Chasteen et al., 2009). We therefore compared the sensitivity of the parental strain, *sigB* mutant, and complemented strain to exposure to 200 mM tellurite. As shown in Figure 5C, the *sigB* mutant was much more sensitive to tellurite than the parental and complemented strains in both 630Δ*erm* and R20291 backgrounds. Bacterial detoxification of tellurite also leads to formation of insoluble tellurium (Te), appearing as black deposits in the plates (Hullo et al., 2010). In disk diffusion assays, we found that the black deposit was less opaque in the *sigB* mutant than in the parental and complemented strains (Fig 5D). The increased sensitivity of the *sigB* mutant to tellurite may be due to the combined action of several mechanisms: i) a drop of the synthesis of tellurium resistance proteins, ii) a down-regulation of genes involved in import and production of cysteine (see below), a compound promoting the formation of tellurium (Hullo et al., 2010), and iii) a reduced resistance to oxidative stress induced by the strong oxidizing ability of tellurite (Chasteen et al., 2009).

The function of σ^B in the management of O_2 tolerance.

Recent studies revealed that bacteria can be exposed to low oxygen (O_2) tension along the gut, and that this tension increases when bacteria get closer to epithelial cells (Marteyn et al., 2011). Thus, during gut colonisation, *C. difficile* is likely to be exposed to a low but toxic O_2 concentration for this strict anaerobe. Incidentally, the enzymes involved in the ROS reduction pathway also participate in O_2 detoxification in *C. acetobutylicum* (Riebe et al., 2009). Because the genes encoding proteins of this detoxification pathway are controlled by σ^B, we sought to determine whether σ^B plays a role in O_2 tolerance in *C. difficile*. We first tested the effect of σ^B inactivation on the growth of *C. difficile* strains in TY soft agar tubes incubated in the presence of air for 24 h. The zone of growth inhibition was significantly taller for the *sigB* mutant than for the parental strain in both 630Δ*erm* and R20291 genetic backgrounds (Fig 6A and 6B). Complementation of the *sigB* mutants restored the phenotype observed in the wild-type strains.

To determine the level of O_2 tension supported by *C. difficile* and to confirm the involvement of σ^B in O_2 tolerance, we monitored the growth of the 630Δ*erm* and R20291 strains, their respective *sigB* mutants, and the complemented strains when exposed to various levels of O_2 tension. For this purpose, we spotted serial dilutions (from 10^0 to 10^{-5}) of each strain on TY plates that we incubated in anaerobiosis or in the presence of 0.1%, 0.4%, or 1% of O_2. All the strains tested were unable to grow in the presence of 1% of O_2 (data not shown). By contrast, in the presence of 0.1% or 0.4% of O_2, the *sigB* mutants showed a drastic growth defect as compared to the parental or complemented strains (Fig 6C). We found that only the first dilutions of the R20291 strain grew in the presence of 0.4% or 0.1% of O_2 as compared to the growth of all dilutions of the 630Δ*erm* strain. This result suggesting that the R20291 strain was more sensitive to O_2 than the 630Δ*erm* strain is consistent with recent studies (Edwards et al., 2016). In addition, the complemented strain in the R20291 genetic background showed higher tolerance to O_2 than the parental strain did at 0.1% and 0.4% of O_2. This result is probably due to the multicopy plasmid used in the complemented strain leading to 30-fold overexpression of *sigB* as detected by qRT-PCR (Table S6). This overexpression may be responsible for the increased protection from O_2. Some clostridia such as *Clostridium butyricum*, can resume growth after exposure to O_2 by consuming O_2 without any lasting damage (Kawasaki, 1998). Multi-enzymatic NAD(P)H oxidase activity, responsible for O_2 consumption by means of either NADH or NADPH, is detected in several clostridia (Kawasaki, 1998), pointing to a common mechanism of defence against O_2; this mechanism is likely functional in *C. difficile*.

Besides, expression of as many as 98 genes is induced when *C. difficile* is exposed to air (Emerson et al., 2008). Among them, 37 are positively controlled by σ^B (Table 1), in line with the phenotype of high sensitivity to O_2 observed in the *sigB* mutant. This set includes rubredoxin-oxidoreductases (*CD1623* and *CD0176*) and two reverse-rubrerythrins (*CD1524* and *CD1474*), in addition to genes involved in thiol homeostasis (see below) and DNA repair (*uvr*) likely involved in protection from O_2 and ROS. The genes are also induced after O_2 exposure in *C. acetobutylicum* (Hillmann et al., 2009a). These observations highlight the strong oxidizing power of O_2 for obligate anaerobic bacteria and the different mechanisms used by these bacteria to overcome the multiple types of damage. Both phenotypic and transcriptomic analyses indicate that σ^B plays a central role in the process of protection from

O_2 by positively controlling the expression of genes implicated in O_2 detoxification pathways or in the repair of damage induced by this compound. To date, σ^B has been characterised only in aerobic firmicutes. We demonstrated for the first time an original and crucial role of σ^B in tolerance of low tension of O_2. This role is currently restricted to a few anaerobic clostridia possessing σ^B.

Involvement of σ^B in the control of thiol homeostasis.

Thiols play pivotal roles in cellular redox homeostasis and are among the first targets of oxidative agents like ROS, NO, and RNS, in addition to O_2. Indeed, the thiol-containing amino acid cysteine is highly sensitive to oxidation, and its reduction and protection are crucial for the cell. In our transcriptome data, genes coding for proteins involved in thiol protection such as one of the thioredoxins (*trxA-CD1690*), the thiol-peroxidase (*CD1822*), the methionine sulfoxide reductase (*msrAB-CD2166*), and a protein annotated as a putative CoASH-reductase (*CD1797*) were down-regulated in the *sigB* mutant compared to the 630Δ*erm* strain (Table 1). When we tested whether the reduced expression of these genes leads to increased sensitivity to diamide, an oxidizing agent specifically targeting thiols, we did not observe significant differences between the *sigB* mutant and the parental strain under our conditions (Fig S7A). However, two different systems composed of a thioredoxin and a thioredoxin reductase are present in the *C. difficile* genome. One expressed under the control of σ^B is probably induced in response to stress, while the other (*CD2117* and *CD3033*) seems to be constitutively expressed. In a rich medium containing peptides and likely cysteine, the control of only one *trx* system (*CD1690-91*) by σ^B may not be sufficient to detect a change in sensitivity to diamide in the *sigB* mutant.

Among thiol molecules, Fe-S clusters are a prime target of oxidizing agents (Py et al., 2011). Of note, σ^B positively controls several genes encoding proteins involved in Fe-S cluster assembly (CD3607) or in the biogenesis of Fe-S clusters, e.g. cysteine desulfurases (CD1279 and CD3670) and a NifU-type protein (CD1280). In addition, we found that the expression of genes involved in cysteine synthesis (*CD1594*) or encoding transporters of cysteine/cystine and sulfonates, which are sulphur compounds leading to cysteine production (Table 1 and Fig S4) (Dubois et al., 2016) also decreased in the *sigB* mutant. Given that cysteine is the direct precursor of Fe-S clusters and because many of the proteins involved in electron transfer, including some of the enzymes of O_2/ROS/NO detoxification, contain Fe-S clusters, the coordinated regulation of both Fe-S cluster biogenesis and cysteine synthesis by σ^B may allow for the supply of cysteine required for Fe-S synthesis and for better protection under oxidative stress (Py et al., 2011). Accordingly, when a reducing agent such as cysteine or thioglycolate was added to air-exposed culture, the growth inhibition was attenuated for all strains (Fig S7B and S7C), suggesting that cysteine or thioglycolate protects thiols from the oxidizing effects of air. These results suggest that σ^B plays an important role in thiol homeostasis and biogenesis of Fe-S clusters, which are crucial for anaerobic metabolism (Meyer, 2000).

Gut colonisation efficiency of the *sigB* mutant in a murine dixenic model.

According to phenotypes and transcriptomic analysis, σ^B is involved both in the response to stresses that *C. difficile* cells may encounter during the infection process and in the control of the expression of several genes encoding proteins likely participating in interactions with host cells. In contrast, σ^B is not involved in the control of toxin production. Consequently, we chose to compare the ability of the *sigB* mutant and wild-type strain to colonise the intestinal tract. To this end, we used a *C. difficile* dixenic mouse model of colonisation (Spigaglia et al., 2013) allowing for moderate host inflammation and a partial immune response (Onderdonk et al., 1980; Souza et al., 2004). We observed no fitness difference between the *sigB* mutant and the wild-type strain during growth in co-culture in TY medium *in vitro* and no difference in germination efficiency. To prevent vegetative cells of the *sigB* mutant from getting killed by air exposure, we infected the mice with an approximately equivalent amount (1:1) of purified spores of the 630Δ*erm* strain and of the s*igB* mutant. The bacterial burden was quantified by seeding caecal and faecal samples on selective plates from day 2 until day 15 post-infection. The 630Δ*erm* strain proliferated in the mice as previously described (Pantaleon et al., 2015), reaching a bacterial burden of infection of 5×10^8 bacteria per gram of faeces after 2 days of infection (Fig 7A). At the same time, the *sigB* mutant showed a 3-log fold decreased burden in the faecal content suggesting a defect in colonisation fitness of this mutant when it competed with the 630Δ*erm* strain (Fig 7A). Although the wild-type strain showed quite a constant amount of bacteria until 15 days post-infection, the colonisation by the *sigB* mutant gradually decreased until the end of the experiment, reaching a 5-log fold lower burden than that of the 630Δ*erm* strain (Fig 7A). Similar results were obtained for the caecal-lumen contents: a 3- and 5-log fold difference in bacterial burden between the 630Δ*erm* strain and the *sigB* mutant after 2 and 15 days of infection, respectively (Fig 7B). We also enumerated the bacterial cells that could be associated with the caecal mucosa. We found $\sim 10^5$ bacteria per gram of caecal mucosa for the wild-type strain (Fig 7C). Furthermore, we observed few if any colonies of the *sigB* mutant indicating a major defect in its association with the caecal mucosa during the infectious cycle. This finding suggests that σ^B might control factors favouring implantation of *C. difficile* associated with the caecal mucosa. Accordingly, we found that σ^B positively controls genes encoding surface-associated proteins that may be involved in adhesion to epithelial cells or to extracellular-matrix components. Among these genes, four genes, *slpA*, *cwp27/CD0440*, *cwp19/CD2767* and *CD3145* are expressed early during colonisation in axenic mice, and their expression decreases at a late stage of infection, suggesting that these genes may be involved in the early stage of colonisation (Janoir et al., 2013).

Sporulation is rapidly induced during the colonisation process in axenic mice (Janoir et al., 2013). Therefore, we monitored the number of spores in faecal and caecal contents as well as in the caecal mucosa (Fig S8). Although our results revealed that the *sigB* mutant produced 10-fold more spores than the wild-type strain did *in vitro*, we observed a reduction in the number of spores formed *in vivo* by the *sigB* mutant compared to the wild-type strain. This result can probably be explained by the rapid elimination of the vegetative cells of the *sigB* mutant since the beginning of infection, thus preventing the sporulation process.

Several hypotheses may explain the huge defect in the *sigB* mutant in terms of colonisation of the gut. Because the rate of spore germination *in vitro* is almost the same between the wild-type and *sigB* mutant strains, it seems unlikely that such a defect can be related to a difference in *in vivo* germination efficiency. In several firmicutes including *C. difficile*, σ^B contributes to the regulation of metabolic function; this regulation can favour adaptation and survival of bacteria when exposed to changing or complex environments like those of the gastrointestinal tract. However, the genes involved in metabolism and up-regulated *in vivo* in axenic mice (Janoir et al., 2013), e.g. sorbitol, ethanolamine, and N-acetyl-glucosamine catabolic pathways, are not controlled by σ^B according to transcriptome data. Moreover, it was recently shown that glutamate utilisation is necessary for *in vivo* colonisation of a hamster model by *C. difficile* (Girinathan et al., 2016). Interestingly, the *gluD* gene encoding a NAD-specific glutamate dehydrogenase involved in glutamate catabolism is positively controlled by σ^B, indicating the probable importance of σ^B for metabolic adaptation during the infection process. However, it seems unlikely that the decrease in the expression of *gluD* in a *sigB* mutant is sufficient to explain the drastic defect in colonisation in our model of co-infection. Indeed, the co-infection of a hamster with the *gluD* mutant and the parental strain partially restores gut colonisation of the mutant, suggesting that production and secretion of this enzyme by the parental strain is sufficient to support the growth of the mutant *in vivo*. The mechanisms behind the stress response, such as those contributing to resistance to host defences and facilitating the persistence of *C. difficile,* most likely favour colonisation. Thus, the reduced ability of the *sigB* mutant to face acidification of its environment probably affects the colonisation efficiency of this mutant. Even if the lack of a microbiota lowers the magnitude of the inflammatory response in axenic mice, the absence of σ^B probably prevents the protection of the bacteria from ROS and RNS produced by the host during inflammation (Abt et al., 2016; Jose and Madan, 2016) and this situation should contribute to the reduced ability of the *sigB* mutant to colonise the gut. It is noteworthy that these different hypotheses are not mutually exclusive and that the severe impairment of the capacity for intestinal-tract colonisation in the *sigB* mutant is a multi-factorial phenomenon.

In pathogenic firmicutes, σ^B is also implicated in colonisation and virulence. Indeed, a *sigB*-null mutant of *Bacillus anthracis* is less virulent in a mouse model (Guldimann et al., 2016). Moreover, σ^B acts as a regulator of virulence in *S. aureus* and is involved in the emergence of small-colony variants (Tuchscherr and Loffler, 2016). In *L. monocytogenes*, the role of σ^B is rather clear because a *sigB* mutant causes attenuated oral infection in a guinea pig model and is less invasive in CaCo-2 cells (Guldimann et al., 2016). This decrease in virulence and in colonisation capacity may be explained by two mechanisms acting either separately or in association, i.e. i) the inability of the *sigB* mutant to adapt to changing environmental conditions or to the exposure to antimicrobial compounds inside the host or ii) the positive or negative control of virulence or pathogenesis factors by σ^B (Guldimann et al., 2016).

Consensus definition and identification of potential direct target genes of σ^B.

According to our transcriptome analysis, σ^B positively controls 410 genes. To identify the genes that are directly transcribed by the RNA polymerase associated with σ^B, we used the genome-wide transcription start site (TSS) mapping described recently (Soutourina et al., 2013) and analysed the sequence upstream of the TSS of genes positively controlled by σ^B. We first found a GGGTATA motif at position -10 and GTTT at position -33 upstream of the TSS of several genes involved in stress response (*CD1524*, *CD1474*, *CD1623*, *trxA*, *msrAB*, and *norV*) (Table 2). These two sequences are rather similar to the consensus sequence recognised by σ^B in *B. subtilis* or *L. monocytogenes* (Petersohn et al., 2001; Kazmierczak et al., 2003). Then, when we looked for all genes positively controlled by σ^B, we found that 20 genes have a similar pattern in their promoter (Table 2). This situation allowed us to propose a consensus sequence WGWTT-$N_{13\text{-}17}$-(G/T)GGTAWA for σ^B-dependent promoters in *C. difficile* (Fig 8). We searched for it in the 300-bp region upstream of the translation start site of *C. difficile* genes on the GenoList web server, allowing two mismatches in the search settings. Among the genes that contain a consensus sequence of σ^B, 27 are positively controlled by σ^B according to our transcriptome data (Table S7). Incidentally, a potential σ^B-dependent promoter was found upstream of the *bcp* gene (encoding a thiol peroxidase), upstream of the *CD0174* operon (encoding an oxidoreductase potentially involved in ROS/O_2 detoxification), and upstream of the *isc2* gene, which encodes a cysteine desulfurase involved in Fe-S cluster biogenesis. In conclusion, most genes involved in ROS, O_2, or NO detoxification pathways or in repair of thiols or DNA have a σ^B-dependent promoter identified either by TSS mapping or *in silico* (Table 2 and Table S7).

It is worth noting that several genes with a promoter containing a consensus sequence probably recognised by σ^B are either not controlled or only slightly controlled by σ^B. This state of affairs may be explained by the fact that our transcriptome was obtained without stress exposure, which is liable to activate σ^B, and some σ^B targets may not be detected under these conditions. Conversely, we did not find a σ^B consensus sequence upstream of all the genes positively controlled by σ^B. This finding can be due to i) an indirect effect of σ^B, ii) the established consensus that needs to be refined, or iii) the degenerate sequences of the consensus recognised by σ^B in *C. difficile*, as shown for sporulation σ factors (Saujet et al., 2013).

Conclusion

In this work, we showed that σ^B performs a crucial function in the physiology of *C. difficile* by controlling ~25% of genes involved in diverse cellular processes at the onset of the stationary phase. Accordingly, we observed a drop in survival of the *sigB* mutant during the stationary phase when the cells face more stressful conditions. Thus, σ^B together with σ^H, which controls ~49% of the genes induced at the onset of the stationary phase (Saujet et al., 2011), are the major actors in decision making during post-exponential growth. It is worth mentioning that most of the genes up-regulated in the stationary phase likely involved in oxidative- and nitrosative-stress responses are controlled by σ^B but not by σ^H (Saujet et al., 2011). On the contrary, σ^H represses the transcription of the toxin genes, whereas σ^B does not play any role in toxinogenesis. Moreover, σ^B and σ^H inversely control the sporulation process. Thus, to face stressful environments encountered during infection, *C. difficile* may use two strategies: a rapid adaptive response to stress stimuli mediated by σ^B or an irreversible and slower differentiation process leading to the formation of spores, whose initiation is under the control of σ^H. Spore formation protects the cells from stresses and enables long-term persistence and dissemination in the environment. The molecular mechanisms that interconnect these two mutually exclusive adaptive responses have yet to be determined. Even though σ^B is involved in several stress responses, we noticed that, unexpectedly, σ^B does not control biofilm formation, known as another strategy to face harmful environments. However, we cannot rule out that σ^B participates in stress resistance inside biofilms as demonstrated for *L. monocytogenes* (van der Veen and Abee, 2010). Accordingly, it has been shown that *C. difficile* cells within a biofilm are protected from O_2 (Dawson et al., 2012), a stress response mediated by σ^B.

CDI is characterised by intense local inflammation in the colon, a process triggered by the surface layer and flagellin and by damage to enterocytes resulting from TcdA and TcdB activities (Abt et al., 2016). Production of pro-inflammatory chemokines and cytokines elicits major infiltration by host immune cells like neutrophils, which will secrete bactericidal compounds such as ROS, NO or antimicrobial peptides (Abt et al., 2016). We showed that σ^B is necessary for expression of genes contributing to resistance to these harmful compounds. Indeed, σ^B inactivation led to higher sensitivity of *C. difficile* to adverse conditions including acidic pH, ROS, NO and O_2 exposure. The specific functions regulated by σ^B vary considerably among species, and the σ^B regulon has probably evolved to facilitate survival in specific environments. The involvement of σ^B in the resistance to ROS and to acidic pH is rather conserved among the firmicutes while its involvement in the ability to resist NO/RNS stress seems to be more specific for *C. difficile*. Moreover, regulators NsrR and SrrAB involved in an NO stress response in *B. subtilis* and *S. aureus*, respectively, are absent in *C. difficile.* The recruitment of σ^B to directly manage NO stress (detoxification, protection and repair) may be related to the intense inflammatory reaction triggered during CDI.

The presence of O_2 is also a major stress for anaerobes. Several pieces of evidence suggest that *C. difficile* vegetative cells may be exposed to O_2 during CDI. Indeed, recent reports indicated that antibiotic treatments may lead to an increase in O_2 tension in the gut by depleting butyrate-producing clostridia facilitating proliferation of aerobic and facultative anaerobic pathogens (Lawley et al., 2012; Rivera-Chavez et al., 2016). Some vegetative cells of *C. difficile* may also be associated with the mucus in the intestinal tract, where O_2 tension is higher than in the lumen (Buckley et al., 2011; Semenyuk et al., 2015). We showed in this work that *C. difficile* can tolerate O_2 concentrations below 1% and that σ^B plays a crucial role in this tolerance through the direct control of genes encoding proteins involved in the O_2 detoxification pathway in other anaerobes (Riebe et al., 2009). Because the general stress response has been studied only in aerobic firmicutes, the present study is the first demonstration of the involvement of σ^B in O_2 tolerance. In *C. acetobutylicum*, in which *sigB* is absent, the PerR repressor, which senses H_2O_2 as a signal of oxygenation (Hillmann et al., 2008; Hillmann et al., 2009a), controls these pathways, whereas its inactivation increases the survival of *C. acetobutylicum* in the presence of O_2 and H_2O_2. At least two regulators intended to manage an O_2/H_2O_2 stress response exist in clostridia (Hillmann et al., 2009a). It is intriguing that a *perR* gene is present in the *C. difficile* genome. PerR may contribute to the control of O_2/ROS detoxification in addition to σ^B or is involved in the regulation of other target genes in response to the presence of H_2O_2.

σ^B does not control toxinogenesis, but our co-infection experiments in axenic mice highlight the crucial role of σ^B in the colonisation process with a drastic decrease in the number of cells of the *sigB* mutant compared to the wild-type strain in faecal and caecal contents. This finding indicates that σ^B serves as a key regulator of gut colonisation by coordinating several processes likely required for adaptation and survival of bacteria within the gut. As mentioned above, σ^B controls and/or transcribes several genes involved in the management of stresses likely encounter by *C. difficile* inside the host. σ^B also induces rerouting of central metabolism. This reprogramming of metabolism can protect the bacterium from acidic pH encountered in an inflamed gut (Nugent et al., 2001). σ^B also controls thiol homeostasis and Fe-S biogenesis, which are important for maintenance of the metabolic activity of anaerobes (Meyer, 2000) and for counteracting the effects of oxidizing compounds. The increased sensitivity of the *sigB* mutant to CAMPs also suggests that σ^B may contribute to the evasion of host innate defences involving antimicrobial peptides. Finally, the positive control by σ^B of genes encoding several cell surface-associated proteins induced during the early steps of colonisation (Janoir et al., 2013) or involved in adhesion to epithelial cells or to extracellular-matrix components (Janoir, 2016) combined with the failure to detect the *sigB* mutant in the caecal mucosa suggest that σ^B may contribute to the ability of *C. difficile* to adhere to the intestinal-tract cells. Accordingly, environmental stress signals have been shown to increase adherence of *C. difficile* strains to Vero cells (Waligora et al., 1999). Altogether, these data strongly support the global involvement of σ^B in a multi-factorial manner in the colonisation of a niche (the intestinal tract) and in the management of the main stresses encountered during CDI.

The σ^B activation in response to environmental stimuli depends on the phosphorylated/ dephosphorylated state of the anti-σ factor RsbV. In *B. subtilis* or *L. monocytogenes*, stressful stimuli such as ethanol, heat, acidification, or depletion of energy are transmitted to the PP2C phosphatase(s) responsible for the dephosphorylation of RsbV that will capture RsbW, leading to the release and activation of σ^B. It is noteworthy that two PP2C phosphatases are encoded in the *C. difficile* genome: SpoIIE (likely involved in the sporulation process) and

CD2685. Among the stresses encountered during the infection process, the stimuli that trigger σ^B activation in *C. difficile* have yet to be identified. Further studies are needed to decipher the signal transduction pathway leading to σ^B activation in *C. difficile* and to better characterise the functions under the control of σ^B that are crucial for gut colonisation.

Experimental procedures.

Bacterial strains and growth conditions.

C. difficile strains and plasmids used in this study are presented in Table S8. *C. difficile* strains were grown anaerobically (5% of H_2, 5% of CO_2, and 90% of N_2) in a TY medium (Bacto tryptone 30 g·l^{-1}, yeast extract 20 g·l^{-1}, pH 7.4), in a BHI medium (Difco), or in a sporulation medium (SM) (Wilson et al., 1982), which was used for sporulation assays. BHI medium supplemented with yeast extract (5 mg·ml^{-1}) and L-cysteine (0.1%) (BHIS) was used for germination and biofilm formation assays. An SMC medium, containing (per litre) 90 g of Bacto™ peptone (Bacto™ 211677), 5 g of Proteose peptone (82450, Sigma-Aldrich), 1 g of $(NH_4)_2SO_4$, and 1.5 g of Tris-(hydroxymethyl) aminomethane, was used to produce spores (Permpoonpattana et al., 2011). Some assays of oxidative-stress resistance of *C. difficile* on plates were performed using a peptone-containing medium (Pep-M) (Ng et al., 2013). This medium contained (per litre) 40 g of Proteose peptone No. 2 (BD Diagnostics, USA), 5 g of Na_2HPO_4, 1 g of KH_2PO_4, 2 g of NaCl, and 0.1 g of $MgSO_4$. Agar was added to a final concentration of 15 g·l^{-1}. When necessary, cefoxitin (Cfx, 25 μg·ml^{-1}), thiamphenicol (Tm, 15 μg·ml^{-1}), erythromycin (Erm, 2.5 μg·ml^{-1}), or lincomycin (Lin, 20 μg·ml^{-1}) were added to *C. difficile* cultures. *E. coli* strains were grown in LB broth. When indicated, ampicillin (100 μg·ml^{-1}) or chloramphenicol (15 μg·ml^{-1}) was added to the culture medium. All routine plasmid construction procedures were carried out by standard methods. All primers used in this study are listed in Table S9.

Construction of *C. difficile* strains.

The ClosTron gene knockout system (Heap et al., 2007; Heap et al., 2009) was used to inactivate the *sigB* gene (*CD0011*) in both 630Δ*erm* and R20291, yielding respectively strains 630Δ*erm sigB::erm* (CDIP229) and R20291 *sigB::erm* (CDIP502). Primers to retarget the group II intron of pMTL0007 to insert it into the *sigB* gene in sense orientation immediately after the 33rd nucleotide in the coding sequence (Table S9) were designed in the Targetron design software (Sigma-Aldrich). The PCR product generated by overlap extension that can facilitate intron retargeting to *sigB* was cloned between the HindIII and BsrG1 sites of pMTL007 to obtain pDIA5959. *E. coli* HB101(RP4) containing pDIA5959 was mated with *C. difficile* 630Δ*erm* and R20291 yielding strains CDIP229 and CDIP502, respectively (Table S8). *C. difficile* transconjugants were selected by sub-culturing on BHI agar containing Tm and Cfx and then plated on BHI agar containing either Erm for 630Δ*erm* or Lin for R20291. Chromosomal DNA of transconjugants was isolated as previously described (Antunes et al., 2011). Several PCRs were realized to verify the integration of the intron into the *sigB* gene and the splicing of the group I intron from the group II intron after integration (Fig S1 and Table S9). To complement the *sigB* mutants, the *sigB* gene (positions -59 to +811 from the translational start site) was amplified by PCR using oligonucleotides IMV705 and IMV704. The PCR product was first cloned between the StuI and BamHI sites into plasmid pDIA6103, a derivative of pRPF185 (Fagan and Fairweather, 2011; Soutourina et al., 2013) to produce pDIA6306. Then, the *sigB* promoter region located upstream of *CD0007*, the first gene of the *CD0007-08-rsbVW-sigB* operon, was amplified by PCR using oligonucleotides IMV711 and IMV712. The PCR fragment was cloned at the KpnI and StuI sites into pDIA6306 to produce pDIA6325. In this plasmid, the P_{sigB} promoter region replaced the P_{tet} promoter present in pDIA6306. This plasmid was transferred by conjugation into the *C. difficile sigB* mutants obtained in the 630Δ*erm* and R20291 backgrounds yielding strains CDIP547 and CDIP505, respectively (Table S8).

Oxidative-stress tolerance assays.

Inhibition of growth by air was tested in soft agar tubes (Rocha et al., 2007). 20 µl of an overnight culture of *C. difficile* grown anaerobically in the TY medium was mixed with 10 ml of TY medium containing 0.4% of agar at 45°C in a screw cap tube. The tubes were then incubated aerobically at 30°C for 24 h. We measured the area from the top of the agar to the edge of visible bacterial growth, considered the zone of growth inhibition by air. Disk diffusion assays were conducted as follows: overnight cultures of strains grown in the Pep-M medium were diluted to an OD_{600nm} of 0.3. The diluted culture (3 ml) was plated on calibrated Pep-M agar. After absorption for 1 h, the excess of culture was removed and the plates were dried for 1 h at 37°C. A sterile 6-mm paper disk was placed on the agar surface and 10 µl of 1 M hydrogen peroxide (H_2O_2), 200 mM tellurite, or 2 M paraquat (methyl-viologen) was added to the disk. The diameter of the growth inhibition was measured after 36 h of incubation at 37°C in the H_2O_2 and tellurite stress assays and 48 h in the paraquat stress assay.

Spotted dilution assays.

Acid, O_2, and NO stress assays were performed as indicated below. Five microliters of different serial dilutions (from 10^0 to 10^{-5}) of *C. difficile* strains grown for 8 h in the TY medium were spotted i) on plates containing TY agar at different pH (4.5, 5, 5.5, 6, or 6.5), ii) on TY plates incubated in the presence of 0.1%, 0.4%, or 1% O_2 tension, or iii) on TY plates containing different concentrations of DEA/NO (250 and 500 µM) or SNP (200 and 500 µM). The last dilution allowing for growth was recorded after incubation at 37°C for 24 h for the assays dealing with acid and NO stress and for 64 h for the low O_2 tension stress.

Nitrosative-stress assays.

Growth of *C. difficile* strains in the TY medium in the presence of DEA/NO was followed using a GloMax® Explorer plate-reader (Promega). Overnight cultures were diluted 50-fold in 1 ml of the TY medium supplemented with 0, 5, or 10 µM DEA/NO and 0, 10, or 20 µM SNP. OD_{600nm} was monitored every hour at 37°C. For survival experiments, 10 ml of the TY medium was inoculated with an overnight culture at OD_{600nm} of 0.05. After 4 h of incubation at 37°C, the cultures were split into two samples of 5 ml. Concentration of either DEA/NO (25 µM) or SNP (40 µM) was added to one of the cultures. After 30 min of incubation, the cells were serially diluted with the TY medium and viability was assessed by growth on TY agar plates for 24 h. The survival rate was determined as the ratio of the number of cfu·ml^{-1} after stress exposure to the total number of cfu·ml^{-1} in the absence of stress exposure.

Assays of sensitivity to antibiotics and antimicrobial peptides.

For the mitomycin C and rifampicin stress assays, 10 ml of the TY medium was inoculated at OD_{600nm} of 0.05 with an overnight culture. After 3 h of incubation at 37°C, stress assays were carried out as described above. 10 µl of mitomycin C (100 µg·ml^{-1}), rifampicin (25 µg·ml^{-1}), or vancomycin (30 µg·ml^{-1}) was added to the disk. The diameter of the growth inhibition was measured after 24 h of incubation at 37°C. To determine the mutation rate of the strains, overnight culture was plated on BHI agar or BHI agar containing 6 µg·ml^{-1} ciprofloxacin. Mutation rates were calculated as the ratio of the colony-forming unit (cfu) per ml on BHI agar with ciprofloxacine to the cfu·ml^{-1} on BHI agar.

Sensitivity assays were performed in the BHI medium in 24-well microplates. Each well was inoculated with 1 ml of a fresh BHI bacterial inoculum at OD_{600nm} of 0.01. The medium was supplemented with a range of concentrations of bacitracin (Sigma Aldrich, ≥ 50000 USP g^{-1}), polymyxin B (Sigma Aldrich, ≥ 6000 USP mg^{-1}), or hen egg white lysozyme. The microplates were incubated at 37°C for 20 h under anaerobic conditions. MIC was defined as the lowest concentration of antimicrobial peptides or lysozyme that prevented growth.

Stationary phase survival, sporulation and germination assays.

For the stationary phase survival test, 10 ml of the TY medium was inoculated at OD_{600nm} of 0.05 with an overnight culture. After 24, 48, and 72 h, serial dilutions were plated on TY agar and incubated for 24 h at 37°C. $Cfu{\cdot}ml^{-1}$ were counted; using the number of $cfu{\cdot}ml^{-1}$ after 24 h of culture as a reference, we measured the survival rate as the ratio of the number of $cfu{\cdot}ml^{-1}$ after each time point of culture to the number of $cfu.ml^{-1}$ after 24 h of cultivation.

Sporulation assays were performed in SM medium after 72 h of growth as previously described (Saujet et al., 2013). The sporulation rate was determined as the ratio of the number of $spores{\cdot}ml^{-1}$ to the total number of $cfu.ml^{-1}$. Spores were purified using the SMC medium. A total of 100 µl of the culture was plated on SMC plates, and the bacteria were grown anaerobically at 37°C for 7 days. Spores were then scraped off with water and incubated for 7 days at 4°C. Cell fragments and spores were separated by centrifugation in a HistoDenz (Sigma-Aldrich) gradient centrifuge (Sorg and Sonenshein, 2009). To determine the germination efficiency, purified spores were resuspended to OD_{600nm} of 1.0 in 4 ml of BHIS supplemented with 1% of taurocholate and 1.3 mM glycine. OD_{600nm} was monitored during anaerobiosis. Data are expressed as the ratio of OD_{600nm} at each time point to OD_{600nm} at time zero (Dembek et al., 2015). Germination was also monitored by phase contrast microscopy.

RNA extraction and quantitative RT-PCR analysis.

Cells were harvested after 10 h of growth in the TY medium. The culture pellets were resuspended in the RNApro solution (MP Biomedicals) and RNA was extracted using the FastRNA Pro Blue Kit. cDNAs synthesis and real-time quantitative PCR were performed as previously described (Saujet et al., 2011; Soutourina et al., 2013). In each sample, the quantity of cDNAs of a gene was normalised to the quantity of cDNAs of the *pgi* and *ccpA* genes. The relative change in gene expression was recorded as the ratio of normalised target concentrations (the threshold cycle [$\Delta\Delta C_T$] method) (Livak and Schmittgen, 2001).

Transcriptome analysis using DNA microarrays.

The microarray analysis of the *C. difficile* 630Δ*erm* transcriptome was designed as previously described (Saujet et al., 2011) (GEO database accession number GPL18319). Transcriptomic analysis was performed using four independent RNA preparations for each 630Δ*erm* and CDIP229 strain. Hybridisation of labelled cDNA to the microarrays and array scanning were conducted as described elsewhere (Saujet et al., 2011). The data were analysed using R and the limma package (Linear Model for Microarray Data) from the Bioconductor project (www.bioconductor.org). We corrected the background by the normexp method, resulting in strictly positive values, and we reduced variability in the log ratios for genes with a weak signal of hybridisation. Then, we normalised each slide by the loess method. To identify differentially expressed genes, we used the Bayesian adjusted *t* statistics and performed the Benjamini-Hochberg multiple-testing correction based on the false discovery rate. A gene was considered differentially expressed when the p-value was <0.05. The complete dataset was deposited in the GEO database under the accession number GSE85981.

Animal models.

All animal experiments in this study were carried out on 6-week-old germfree C3H/He female mice (CNRS, Orléans, France). We checked the germ-free status of each animal by Gram staining of faeces and by inoculating faeces into the BHI medium and by incubating the medium for 48 h, both aerobically and anaerobically. Twelve mice were then co-infected by oral gavage with a mix of equivalent amounts of purified spores of strains 630Δ*erm* and *sigB* mutant ($\sim 5 \times 10^5$ each). Colonisation was followed by enumeration of *C. difficile* cells in faeces sampled throughout the experiment (days 2, 7, 9, 12, and 15 post-infection) on BHI or BHI+Erm agar plates supplemented with 3% of defibrinated horse blood to differentiate the strains. Briefly, faeces were resuspended in PBS at 10 $mg \cdot ml^{-1}$ and were then serially diluted with PBS before plating on BHI agar or BHI+Erm agar. Spores were also enumerated in the same samples. A 500-µl aliquot of each faeces sample (10 $mg \cdot ml^{-1}$) was mixed with 500 µl of 96% ethanol and incubated for 30 min at room temperature. The samples were centrifuged for 10 min at 5000 rpm, and the pellets were resuspended in 1 ml of PBS and serially diluted before plating on BHI agar or BHI+Erm agar containing 0.1% of taurocholate. The plates were incubated for 48 h anaerobically at 37°C. Four mice were euthanized by cervical dislocation on days 2, 7, and 15. Burdens of vegetative cells and spores of *C. difficile* in the caecal content of each mouse were analysed by selective plating on BHI agar as described above. Finally, the caecal mucosa was washed twice with PBS, dried on a sterile absorbent paper, and ground in an ultraTurrax apparatus (IKA-Labortechnik) for 1 min at 13 500 rpm in 10 ml of PBS supplemented with 10 µl of 10% Tween 80. Caecal-mucosa-associated bacteria (vegetative cells and spores) were then enumerated as described above. All animal experiments were conducted according to the European Union guidelines for the handling of laboratory animals (http://ec.europa.eu/environment/chemicals/lab_animals/home_en.htm). Procedures for infection, euthanasia, and specimen collection were approved by the Central Animal Care Facilities and Use Committee of University Paris-Sud (agreement 92-019-01; protocol number 2012-107).

Acknowledgments

We are thankful to Thomas Dubois and Al Claiborne for helpful discussions and to Jovana Mihajlovic and Jean-Marc Ghigo for their help with oxygen assays. This work was funded by the Institut Pasteur and the University Paris 7.

Table

Table 1. Genes probably involved in stress response expressed under the control of σ^B

Gene ID	Name	Function	Ratio *sigB*/630Δ*erm* Transcriptome[a]	Promoter[b]	Induced by stress[c]
Oxidative and nitrosative stresses					
*CD0825^*	*rbr*	Rubrerythrin	0.31	σ^A	Acid
CD0827		Desulfoferrodoxin	0.18		-
*CD0828^*		Oxidative stress glutamate synthase	0.19		-
*CD0179^*	*gluD*	NAD-specific glutamate dehydrogenase	0.36		-
CD1474		Reverse rubrerythrin (Rr)	0.05	σ^B	Air
CD1524		Reverse rubrerythrin (Rr)	0.05	σ^B	Air
*CD0174^*	*cooS*	CO dehydrogenase	0.01	σ^{B*}	Air
*CD0175^*		Oxidoreductase, Fe-S subunit	0.02		Air
*CD0176^*		Oxidoreductase, NAD/FAD binding subunit	0.02		Air
*CD1623^*		NADH-oxidoreductase	0.13	σ^B	Air
*CD1157^*	*norV*	Anaerobic nitric oxide reductase	0.05	σ^B	Air
*CD2168^*	*hcp*	Hydroxylamine reductase	0.4		
*CD1125^*		Nitroreductase-family protein	0.06	σ^{B*}	Air
*CD0837^*		Putative nitroreductase	0.49	σ^{B*}	Heat
*CD3670^*		Cysteine desulfurase family protein	0.44		
*CD1279^*	*iscS2*	cysteine desulfurase	0.16	σ^{B*}	Amoxicillin
*CD1280^*	*iscU*	Putative NifU-like protein	0.16		
CD3607		Putative iron-sulfur assembly protein	0.5		Amoxicillin
*CD1594^*	*cysK*	O-acetyl-serine thiol-lyase A	0.26		
CD2174		Cyst(e)ine ABC transporter	0.43		Alkali
CD2176		Cyst(e)ine ABC transporter	0.43		Clindamycin
CD2177		Cyst(e)ine ABC transporter	0.48		
CD1482		Sulfonate ABC transporter	0.32		
CD1483		Sulfonate ABC transporter	0.34		

*CD1484^*		Sulfonate ABC transporter	0.14		
CD0999		Sulfonate ABC transporter	0.27		
*CD2166^*	*msrAB*	Methionine sulfoxide reductase	0.5	σ^B	-
*CD1690^*	*trxA*	Thioredoxin	0.5	σ^B	Air
*CD1822^*	*bcp*	Thiol-peroxidase	0.2	σ^{B*}	Acid/Air
*CD1823^*		Unknown function	0.3		-
*CD1796^*		Nitrite and sulfite reductase subunit	0.46	σ^A	Acid/Air
*CD1797^*		CoA disulfide reductase	0.47		-
Other stress					
CD0900	*opuCA*	ABC transporter, glycine betaine/carnitine/ choline ATP-binding protein	0.14		
CD0901	*opuCC*	ABC transporter, glycine betaine/carnitine/ choline permease	0.19		
CD2252	*eam*	Glutamate 2,3-aminomutase	0.36		
CD3410	*uvrC*	Excinuclease ABC subunit C	0.43	σ^B	Air
CD3411	*uvrA*	Excinuclease ABC subunit A	0.35		
CD3412	*uvrB*	Excinuclease ABC subunit B	0.29	σ^B	
CD1977	*mutS*	DNA mismatch repair protein MutS	0.37		
CD1652		Tellurium resistance protein	0.21		
CD1634	*terD^*	Tellurium resistance protein	0.47		Amoxicillin
CD1635	*terD^*	Tellurium resistance protein	0.41		Clindamycin
CD1636	*terD^*	Tellurium resistance protein	0.63		
CD1639		Tellurite associated resistance protein	0.52		Amoxicillin
CD0558	*glsA*	Glutaminase	0.45	σ^B	
CD1132		Putative heavy-metal transport/ detoxification protein	2.1		Clindamycin
CD3219		Heat shock protein, HSP33	5.92		
CD0193	*groS*	GroES protein	1.9		Acid/Heat
CD0194	*groL*	GroEL protein	1.8		Acid/Heat
Antibiotics					
CD1624	*vanR*	Two-component response regulator	0.41	σ^{B*}	Air
CD1625	*vanS*	Two-component sensor histidine kinase	0.43		
CD2506	*linCd*	Transporter, Major Facilitator Superfamily	0.45		
CD3198	*cme*	Multidrug resistance Cme transporter	2.43		
CD2817		ABC-transporter, multidrug-family	3.92		
CD2818		ABC-transporter, multidrug-family	3.93		
CD0293		ABC-transporter, multidrug-family ATP-binding protein	3.02		
CD0294		ABC-transporter, multidrug-family permease	2.73		
CD1473		ABC-transporter, multidrug-family	2.5		

Gene names and functions correspond to those indicated in the MaGe database Clostriscope (https://www.genoscope.cns.fr). a) A gene was considered as differentially expressed between the strain 630Δ*erm* and the *sigB* mutant when the p-value is < 0.05 using the statistical analysis described in *Experimental procedures*. "^" indicates that the gene is induced at the onset of stationary phase (Saujet et al., 2011). b) the promoters indicated have been mapped in a genome-wide TSS mapping performed with strain 630Δ*erm* (Soutourina et al., 2013). "*" indicates the presence of a *in silico* detected σ^B-dependent promoter (See Table S7). c) the genes differentially expressed in response to various stresses (Emerson et al., 2008) are indicated.

Table 2. Promoters characterised by transcriptional start site mapping with a σ^B consensus sequence.

Gene id	Name	Function	TSS	*sigB*/ 630Δ*erm*	Promoter
CD1474		Reverse rubrerythrin	1709263	0.05	aaa**TTGTTT**aaaggtatatggtgc**GGGTATA**tatagact**A**
CD1524		Reverse rubrerythrin	1766842	0.05	tta**GTGTTT**aagctataaagtctg**GGGTATA**tatattctt**G**
CD1623		NADH-oxidoreductase	1878917	0.13	att**TTGTTT**aaaatataacaagca**GGGTATA**aagagact**A**
CD1690	*trxA*	Thioredoxin	1963153	0.5	aaa**TTGTTT**ttagaaatgaagaat**GGGTATA**ctaattagt**A**
CD2166	*msrAB*	Met sulfoxide reductase	2506476	0.5	atg**CAGATT**attaagttacttctta**GGGAATA**aataaagt**A**
CD1157	*norV*	Putative NO reductase	1356839	0.05	ctt**TTGTTT**cattcacctcaaaatg**GGGTATG**ttacttata**T**
CD0759	*plfB*	Formate acetyltransferase	931482	0.15	tat**TTGTTT**tattttatttatatat**GGGTATA**atttcacc**A**
CD3605.1		Ferredoxin	4213353	0.02	tat**ATGTTT**aaattggtatatat**TGGATAAA**tatctaag**G**
CD2524	*nadD*	Nicotinate-nucleotide adenylyltransferase	2917759	0.49	tat**AAGCTT**taagaaataaaaaataa**TGGTACA**atagtatt**A**
CD3412	*uvrB*	Excinuclease subunit B	3998240	0.29	ttt**TAGATT**taagtaaaatttaaat**GGGTAAA**atattt**A**
CD0668		Two component system	809622	0.45	att**TAGGCA**aagttgtgaaaat**GGGTATA**tggtatact**A**
CD2046		Conserved hypothetical protein	2359093	0.02	aaa**TTGATT**agtacattattaatta**GGGTATA**aaatggtgt**A**
CD0957		Lipoproteine	1125592	0.24	caa**GTGCTT**tgtctgttaaaaaa**TGGTATA**atagagat**A**
CD1451	*folB*	Dihydroneopterin aldolase	1680637	0.4	agt**GTGTAT**aatgcataatcaagat**GGGACAA**actatgac**A**
CD2717		Conserved hypothetical protein	3147779	0.32	tat**AAGTTA**gtacagatattaaaaa**TGGTATA**atataagat**A**
CD0558	*glsA*	Glutaminase	664932	0.45	aca**TTGTTT**tattatagtataaactt**GTGCTAA**aataga**A**
CD1455	*sigA1*	Sigma factor	1684639	0.38	ata**ATGATA**tgaaagaggtaga**TGGTAGA**gttatgg**A**
CD0835		Regulator	1012509	0.44	aa**TTGAAC**tttcaaccaaaata**TGGTAAA**attt**A**
CD2115.1		Conserved hypothetical protein	2447122	0.13	aaa**AACTTT**tataaagtttatattt**GGGTATA**aaagt**A**
CD2321	*tkt'*	Transketolase	2684375	0.5	aaa**AGGTAA**aggtgtttcattta**TGGAAAA**taatgctgc**A**

Genes positively controlled by σ^B whose region around the transcription initiation start site, determined in genome-wide TSS mapping experiment (Soutourina et al., 2013), displays consensus sequence closed to the one present in the promoters recognised by σ^B in other firmicutes. The transcriptional start sites and the -10 and -35 boxes are indicated in bold and in uppercase, respectively. Met : methionine.

Figure legends

Figure 1. Growth and stationary phase survival of the *sigB* mutant.

A) Growth curves of the 630Δ*erm* (black circle) and the 630Δ*erm sigB*::*erm* (dark grey square) grown in TY. These data are the mean with the standard deviations of six independent experiments. B) The histograms represent the percentage of stationary phase survival of the 630Δ*erm* strain (black) and the *sigB* mutant (dark grey) in TY after 24 h, 48 h and 72 h. Survival rate was determined as the ratio of the number of cfu·ml^{-1} after each time point of culture to the number of cfu.ml^{-1} after 24 h of growth. These data are the mean with the standard deviations of 5 independent experiments.

Figure 2. σ^B mediates protection against mitomycin C and rifampicin.

The histograms represent the diameters of the growth inhibition area for the strain 630Δ*erm* (black), the *sigB* mutant (dark grey) or the complemented strain (*sigB* + P_B-*sigB*) (light grey).

Disk diffusion assays were performed with 10 µl of 0.1 $mg.ml^{-1}$ mitomycin C (A) or of 25 $\mu g.ml^{-1}$ rifampicin (B). These results correspond to the mean values with the standard deviations of six and four independent experiments for mitomycin C and rifampicin, respectively. The P-values were 0.0049 for mitomycin C and 0.0256 for rifampicin (Wilcoxon test).

Figure 3. Sensitivity of the *sigB* mutant to acid pH.

An acid stress assay was performed. Serial dilutions of the 630Δ*erm* strain (1), the *sigB* mutant (2) and the complemented strain (*sigB* + P_B-*sigB*) (3) were spotted on TY agar plates at pH 7, 6, 5.5, 5, or 4.5. The plates were incubated 24 h at 37°C. These results are representative of 4 independent experiments.

Figure 4. NO and nitrosative stress sensitivity of the *sigB* mutant.

A) NO and RNS stress assays. Serial dilutions of 630Δ*erm* (1), 630Δ*erm sigB*::*erm* (2) and 630Δ*erm sigB*::*erm* + P_B-*sigB* (3) were spotted on TY plates with different DEA/NO and SNP concentrations. Plates were then incubated 24 h at 37°C. These results are representative of 4 independent experiments. B, C and D) Growth in TY of the 630Δ*erm* strain (black diamonds), the *sigB* mutant (dark grey squares) and the complemented strain (light grey triangles) in presence of 0 (B), 5 (C) or 10 µM (D) of DEA/NO, respectively. The strains were grown at 37°C in a 24-well plate sealed by an adhesive film impermeable to O_2. OD_{600nm} was monitored using a plate-reader every hour after agitation. These data are the mean of five independent experiments. In TY medium containing 5 µM of DEA/NO, the generation time of the *sigB* mutant was 121 min^{-1} compared to 71 min^{-1} and 70 min^{-1} for the 630Δ*erm* strain and the complemented strain, respectively.

Figure 5. Oxidative stress sensitivity of the *sigB* mutant in both the 630Δ*erm* and the R20291 backgrounds.

The histograms represent the diameters of the growth inhibition area of the wild-type strain (black), the *sigB* mutant (dark grey), and the complemented strain (*sigB* + P_B *sigB*, light grey) in the 630Δ*erm* and the R20291 genetic backgrounds. Disk diffusion assays were performed with 1 M H_2O_2 (A), 2 M paraquat (B) and 200 mM tellurite (C, D). Panel D corresponds to plates of a disk diffusion assay with tellurite. Insoluble tellurium forms black halo (Hullo et al., 2010). The data are the mean with the standard deviations of six independent experiments. For the H_2O_2 the P-values were 0.0009 and 0.0047, for the paraquat the P-values were 0.0046 and 0.0047 and for the tellurite experiment, the P-values were 0.0049 and 0.0033 in the 630Δ*erm* and R20291 backgrounds, respectively (Wilcoxon test).

Figure 6. Air and O_2 sensitivity of the *sigB* mutant in the 630Δ*erm* and the R20291 backgrounds.

A and B) Growth of *C. difficile* in the presence of air in soft-agar tubes using a TY medium containing 0.4% agar. A) The histograms represent the distance of growth inhibition between the top of the agar at air interface and the edge of visible bacterial growth for the wild-type (black), the *sigB* mutant (dark grey), and the *sigB* + P_B-*sigB* complemented strain (light grey) in the 630Δ*erm* and the R20291 genetic backgrounds. The data are the mean values with standard deviations of ten independent experiments. The P-values were 7.5 x 10^{-5} and 0.00017 for the 630Δ*erm* and the R20291 genetic backgrounds, respectively (Wilcoxon test). B) The air tolerant assay in soft agar tubes for the R20291 strains. The white arrows indicate the interface between bacterial growth and the zone of growth inhibition. C) Serial dilutions of the wild-type (1 and 4), the *sigB* mutant (2 and 5) and the complemented strain (*sigB* + P_B *sigB*) (3 and 6) in both the 630Δ*erm* (1, 2 and 3) and the R20291 (4, 5 and 6) genetic backgrounds, respectively were spotted on TY + 0.05% taurocholate. The plates were incubated during 64 h either in anaerobic atmosphere (control) or in the presence of 0.1% or 0.4% of O_2. These results are representative of at least five independent experiments.

Figure 7. Impact of *sigB* inactivation on gut colonisation of axenic mice.

Axenic mice were co-infected with an equivalent amount of purified spores of the 630Δ*erm* strain and the *sigB* mutant. Colonisation process and bacterial burden were monitored by seeding both faecal (A) and caecal (B) contents on selective plates (see *Experimental procedures*). A) Total cfu·g faeces^{-1} for both the 630Δ*erm* strain (black) and the *sigB* mutant (light grey) were enumerated in each mouse from day 2 (D2) post-gavage until day 15 (D15) post-gavage. The means of bacterial load in all the mice are shown in dark grey for both strains and each day of enumeration. B) Total cfu·ml^{-1} of caecal content for both the 630Δ*erm* strain (black) and the *sigB* mutant (light grey) were enumerated after sacrifice of four mice after 2 (D2), 7 (D7) and 15 (D15) days post-gavage. The means of bacterial load in all the mice are shown in dark grey for both strains and each day of enumeration. C) Total cfu·g caecal mucosa^{-1} (see *Experimental procedures*) for both the 630Δ*erm* strain and the *sigB* mutant were enumerated after sacrifice of four mice after 2 (D2), 7 (D7) and 15 (D15) days post-gavage. The values are the means of the bacterial burden from the four mice.

Figure 8: **Consensus of σ^B-dependent promoters in *C. difficile*.**

Using an alignment of all the proposed σ^B-dependent promoters mapped listed in Table 3, the sequence logo was created on the WebLogo website (http://weblogo.berkeley.edu). The height of the letters is proportional to their frequency.

References

Abt, M.C., McKenney, P.T., and Pamer, E.G. (2016) *Clostridium difficile* colitis: pathogenesis and host defence. *Nat Rev Microbiol* **14**: 609-620.

Antunes, A., Martin-Verstraete, I., and Dupuy, B. (2011) CcpA-mediated repression of *Clostridium difficile* toxin gene expression. *Mol Microbiol* **79**: 882-899.

Bandow, J.E., Brotz, H., and Hecker, M. (2002) *Bacillus subtilis* tolerance of moderate concentrations of rifampin involves the sigma(B)-dependent general and multiple stress response. *J Bacteriol* **184**: 459-467.

Bischoff, M., Dunman, P., Kormanec, J., Macapagal, D., Murphy, E., Mounts, W. et al. (2004) Microarray-based analysis of the *Staphylococcus aureus* sigmaB regulon. *J Bacteriol* **186**: 4085-4099.

Bruno, J.C., Jr., and Freitag, N.E. (2011) Listeria monocytogenes adapts to long-term stationary phase survival without compromising bacterial virulence. *FEMS Microbiol Lett* **323**: 171-179.

Buckley, A.M., Spencer, J., Candlish, D., Irvine, J.J., and Douce, G.R. (2011) Infection of hamsters with the UK *Clostridium difficile* ribotype 027 outbreak strain R20291. *J Med Microbiol* **60**: 1174-1180.

Cafardi, V., Biagini, M., Martinelli, M., Leuzzi, R., Rubino, J.T., Cantini, F. et al. (2013) Identification of a novel zinc metalloprotease through a global analysis of *Clostridium difficile* extracellular proteins. *PLoS One* **8**: e81306.

Cebrian, G., Sagarzazu, N., Aertsen, A., Pagan, R., Condon, S., and Manas, P. (2009) Role of the alternative sigma factor sigma on *Staphylococcus aureus* resistance to stresses of relevance to food preservation. *J Appl Microbiol* **107**: 187-196.

Chasteen, T.G., Fuentes, D.E., Tantalean, J.C., and Vasquez, C.C. (2009) Tellurite: history, oxidative stress, and molecular mechanisms of resistance. *FEMS Microbiol Rev* **33**: 820-832.

Childress, K.O., Edwards, A.N., Nawrocki, K.L., Woods, E.C., Anderson, S.E., and McBride, S.M. (2016) The Phosphotransfer Protein CD1492 Represses Sporulation Initiation in *Clostridium difficile*. *Infect Immun* **84**.

Cotter, P.D., and Hill, C. (2003) Surviving the acid test: responses of gram-positive bacteria to low pH. *Microbiol Mol Biol Rev* **67**: 429-453, table of contents.

Dawson, L.F., Valiente, E., Faulds-Pain, A., Donahue, E.H., and Wren, B.W. (2012) Characterisation of *Clostridium difficile* biofilm formation, a role for Spo0A. *PLoS One* **7**: e50527.

de Been, M., Francke, C., Siezen, R.J., and Abee, T. (2011) Novel sigmaB regulation modules of Gram-positive bacteria involve the use of complex hybrid histidine kinases. *Microbiology* **157**: 3-12.

Deakin, L.J., Clare, S., Fagan, R.P., Dawson, L.F., Pickard, D.J., West, M.R. et al. (2012) The *Clostridium difficile spo0A* gene is a persistence and transmission factor. *Infect Immun* **80**: 2704-2711.

Dembek, M., Barquist, L., Boinett, C.J., Cain, A.K., Mayho, M., Lawley, T.D. et al. (2015) High-throughput analysis of gene essentiality and sporulation in *Clostridium difficile*. *MBio* **6**: e02383.

Dubois, T., Dancer-Thibonnier, M., Monot, M., Hamiot, A., Bouillaut, L., Soutourina, O. et al. (2016) Control of *Clostridium difficile* Physiopathology in Response to Cysteine Availability. *Infect Immun* **84**: 2389-2405.

Edwards, A.N., Karim, S.T., Pascual, R.A., Jowhar, L.M., Anderson, S.E., and McBride, S.M. (2016) Chemical and Stress Resistances of *Clostridium difficile* Spores and Vegetative Cells. *Front Microbiol* **7**: 1698.

El Meouche, I., Peltier, J., Monot, M., Soutourina, O., Pestel-Caron, M., Dupuy, B., and Pons, J.L. (2013) Characterization of the SigD regulon of *C. difficile* and its positive control of toxin production through the regulation of *tcdR*. *PLoS One* **8**: e83748.

Emerson, J.E., Stabler, R.A., Wren, B.W., and Fairweather, N.F. (2008) Microarray analysis of the transcriptional responses of *Clostridium difficile* to environmental and antibiotic stress. *J Med Microbiol* **57**: 757-764.

Engelmann, S., and Hecker, M. (1996) Impaired oxidative stress resistance of *Bacillus subtilis sigB* mutants and the role of *katA* and *katE*. *FEMS Microbiol Lett* **145**: 63-69.

Entenza, J.M., Moreillon, P., Senn, M.M., Kormanec, J., Dunman, P.M., Berger-Bachi, B. et al. (2005) Role of sigmaB in the expression of *Staphylococcus aureus* cell wall adhesins ClfA and FnbA and contribution to infectivity in a rat model of experimental endocarditis. *Infect Immun* **73**: 990-998.

Ethapa, T., Leuzzi, R., Ng, Y.K., Baban, S.T., Adamo, R., Kuehne, S.A. et al. (2013) Multiple factors modulate biofilm formation by the anaerobic pathogen *Clostridium difficile. J Bacteriol* **195**: 545-555.

Fagan, R.P., and Fairweather, N.F. (2011) *Clostridium difficile* has two parallel and essential Sec secretion systems. *J Biol Chem* **286**: 27483-27493.

Ferreira, A., O'Byrne, C.P., and Boor, K.J. (2001) Role of sigma(B) in heat, ethanol, acid, and oxidative stress resistance and during carbon starvation in *Listeria monocytogenes*. *Appl Environ Microbiol* **67**: 4454-4457.

Fimlaid, K.A., Bond, J.P., Schutz, K.C., Putnam, E.E., Leung, J.M., Lawley, T.D., and Shen, A. (2013) Global analysis of the sporulation pathway of *Clostridium difficile*. *PLoS Genet* **9**: e1003660.

Giachino, P., Engelmann, S., and Bischoff, M. (2001) Sigma(B) activity depends on RsbU in *Staphylococcus aureus*. *J Bacteriol* **183**: 1843-1852.

Girinathan, B.P., Braun, S.E., and Govind, R. (2014) *Clostridium difficile* glutamate dehydrogenase is a secreted enzyme that confers resistance to H2O2. *Microbiology* **160**: 47-55.

Girinathan, B.P., Braun, S., Sirigireddy, A.R., Lopez, J.E., and Govind, R. (2016) Importance of Glutamate Dehydrogenase (GDH) in *Clostridium difficile* Colonization In Vivo. *PLoS One* **11**: e0160107.

Guldimann, C., Boor, K.J., Wiedmann, M., and Guariglia-Oropeza, V. (2016) Resilience in the Face of Uncertainty: Sigma Factor B Fine-Tunes Gene Expression To Support Homeostasis in Gram-Positive Bacteria. *Appl Environ Microbiol* **82**: 4456-4469.

Heap, J.T., Pennington, O.J., Cartman, S.T., and Minton, N.P. (2009) A modular system for Clostridium shuttle plasmids. *J Microbiol Methods* **78**: 79-85.
Heap, J.T., Pennington, O.J., Cartman, S.T., Carter, G.P., and Minton, N.P. (2007) The ClosTron: a universal gene knock-out system for the genus Clostridium. *J Microbiol Methods* **70**: 452-464.
Hecker, M., Pane-Farre, J., and Volker, U. (2007) SigB-dependent general stress response in *Bacillus subtilis* and related gram-positive bacteria. *Annu Rev Microbiol* **61**: 215-236.
Hensbergen, P.J., Klychnikov, O.I., Bakker, D., van Winden, V.J., Ras, N., Kemp, A.C. et al. (2014) A novel secreted metalloprotease (CD2830) from *Clostridium difficile* cleaves specific proline sequences in LPXTG cell surface proteins. *Mol Cell Proteomics* **13**: 1231-1244.
Hillmann, F., Fischer, R.J., Saint-Prix, F., Girbal, L., and Bahl, H. (2008) PerR acts as a switch for oxygen tolerance in the strict anaerobe *Clostridium acetobutylicum*. *Mol Microbiol* **68**: 848-860.
Hillmann, F., Doring, C., Riebe, O., Ehrenreich, A., Fischer, R.J., and Bahl, H. (2009a) The role of PerR in O2-affected gene expression of *Clostridium acetobutylicum*. *J Bacteriol* **191**: 6082-6093.
Hillmann, F., Riebe, O., Fischer, R.J., Mot, A., Caranto, J.D., Kurtz, D.M., Jr., and Bahl, H. (2009b) Reductive dioxygen scavenging by flavo-diiron proteins of *Clostridium acetobutylicum*. *FEBS Lett* **583**: 241-245.
Hochgrafe, F., Wolf, C., Fuchs, S., Liebeke, M., Lalk, M., Engelmann, S., and Hecker, M. (2008) Nitric oxide stress induces different responses but mediates comparable protein thiol protection in *Bacillus subtilis* and *Staphylococcus aureus*. *J Bacteriol* **190**: 4997-5008.
Hullo, M.F., Martin-Verstraete, I., and Soutourina, O. (2010) Complex phenotypes of a mutant inactivated for CymR, the global regulator of cysteine metabolism in *Bacillus subtilis. FEMS Microbiol Lett* **309**: 201-207.
Janoir, C. (2016) Virulence factors of *Clostridium difficile* and their role during infection. *Anaerobe* **37**: 13-24.
Janoir, C., Deneve, C., Bouttier, S., Barbut, F., Hoys, S., Caleechum, L. et al. (2013) Adaptive strategies and pathogenesis of *Clostridium difficile* from in vivo transcriptomics. *Infect Immun* **81**: 3757-3769.
Jose, S., and Madan, R. (2016) Neutrophil-mediated inflammation in the pathogenesis of *Clostridium difficile* infections. *Anaerobe* **41**: 85-90.
Kawasaki, S.N., T.; Nishiyama, Y.; Benno, Y.; Uchilura, T.; Komagata, J.; Kozaki, M.; Niimura, Y. (1998) Effect of oxygen on the growth of *clostridium butyricum* (type of the genus clostridium), and the distribution of enzymes for oxygen and for active oxygen species in clostridia. *J. Fermentation and Bioengineer* **86**: 5.
Kazmierczak, M.J., Mithoe, S.C., Boor, K.J., and Wiedmann, M. (2003) *Listeria monocytogenes* sigma B regulates stress response and virulence functions. *J Bacteriol* **185**: 5722-5734.
Lawley, T.D., Croucher, N.J., Yu, L., Clare, S., Sebaihia, M., Goulding, D. et al. (2009) Proteomic and genomic characterization of highly infectious *Clostridium difficile* 630 spores. *J Bacteriol* **191**: 5377-5386.
Lawley, T.D., Clare, S., Walker, A.W., Stares, M.D., Connor, T.R., Raisen, C. et al. (2012) Targeted restoration of the intestinal microbiota with a simple, defined bacteriotherapy resolves relapsing *Clostridium difficile* disease in mice. *PLoS Pathog* **8**: e1002995.
Livak, K.J., and Schmittgen, T.D. (2001) Analysis of relative gene expression data using real-time quantitative PCR and the 2(-Delta Delta C(T)) Method. *Methods* **25**: 402-408.

Lumppio, H.L., Shenvi, N.V., Summers, A.O., Voordouw, G., and Kurtz, D.M., Jr. (2001) Rubrerythrin and rubredoxin oxidoreductase in *Desulfovibrio vulgaris*: a novel oxidative stress protection system. *J Bacteriol* **183**: 101-108.
Mader, U., Nicolas, P., Depke, M., Pane-Farre, J., Debarbouille, M., van der Kooi-Pol, M.M. et al. (2016) *Staphylococcus aureus* Transcriptome Architecture: From Laboratory to Infection-Mimicking Conditions. *PLoS Genet* **12**: e1005962.
Mani, N., and Dupuy, B. (2001) Regulation of toxin synthesis in *Clostridium difficile* by an alternative RNA polymerase sigma factor. *Proc Natl Acad Sci U S A* **98**: 5844-5849.
Marteyn, B., Scorza, F.B., Sansonetti, P.J., and Tang, C. (2011) Breathing life into pathogens: the influence of oxygen on bacterial virulence and host responses in the gastrointestinal tract. *Cell Microbiol* **13**: 171-176.
McBride, S.M., and Sonenshein, A.L. (2011a) Identification of a genetic locus responsible for antimicrobial peptide resistance in *Clostridium difficile*. *Infect Immun* **79**: 167-176.
McBride, S.M., and Sonenshein, A.L. (2011b) The dlt operon confers resistance to cationic antimicrobial peptides in *Clostridium difficile*. *Microbiology* **157**: 1457-1465.
Meyer, J. (2000) Clostridial iron-sulphur proteins. *J Mol Microbiol Biotechnol* **2**: 9-14.
Mitchell, G., Lamontagne, C.A., Brouillette, E., Grondin, G., Talbot, B.G., Grandbois, M., and Malouin, F. (2008) *Staphylococcus aureus* SigB activity promotes a strong fibronectin-bacterium interaction which may sustain host tissue colonization by small-colony variants isolated from cystic fibrosis patients. *Mol Microbiol* **70**: 1540-1555.
Mols, M., and Abee, T. (2011) *Bacillus cereus* responses to acid stress. *Environ Microbiol* **13**: 2835-2843.
Moore, C.M., Nakano, M.M., Wang, T., Ye, R.W., and Helmann, J.D. (2004) Response of *Bacillus subtilis* to nitric oxide and the nitrosating agent sodium nitroprusside. *J Bacteriol* **186**: 4655-4664.
Nannapaneni, P., Hertwig, F., Depke, M., Hecker, M., Mader, U., Volker, U. et al. (2012) Defining the structure of the general stress regulon of *Bacillus subtilis* using targeted microarray analysis and random forest classification. *Microbiology* **158**: 696-707.
Ng, Y.K., Ehsaan, M., Philip, S., Collery, M.M., Janoir, C., Collignon, A. et al. (2013) Expanding the repertoire of gene tools for precise manipulation of the *Clostridium difficile* genome: allelic exchange using pyrE alleles. *PLoS One* **8**: e56051.
Nugent, S.G., Kumar, D., Rampton, D.S., and Evans, D.F. (2001) Intestinal luminal pH in inflammatory bowel disease: possible determinants and implications for therapy with aminosalicylates and other drugs. *Gut* **48**: 571-577.
O'Byrne, C.P., and Karatzas, K.A. (2008) The role of sigma B (sigma B) in the stress adaptations of *Listeria monocytogenes*: overlaps between stress adaptation and virulence. *Adv Appl Microbiol* **65**: 115-140.
Oliver, A., Baquero, F., and Blazquez, J. (2002) The mismatch repair system (*mutS, mutL* and *uvrD* genes) in *Pseudomonas aeruginosa*: molecular characterization of naturally occurring mutants. *Mol Microbiol* **43**: 1641-1650.
Oliver, H.F., Orsi, R.H., Ponnala, L., Keich, U., Wang, W., Sun, Q. et al. (2009) Deep RNA sequencing of *L. monocytogenes* reveals overlapping and extensive stationary phase and sigma B-dependent transcriptomes, including multiple highly transcribed noncoding RNAs. *BMC Genomics* **10**: 641.
Onderdonk, A.B., Cisneros, R.L., and Bartlett, J.G. (1980) *Clostridium difficile* in gnotobiotic mice. *Infect Immun* **28**: 277-282.
Pantaleon, V., Soavelomandroso, A.P., Bouttier, S., Briandet, R., Roxas, B., Chu, M. et al. (2015) The *Clostridium difficile* Protease Cwp84 Modulates both Biofilm Formation and Cell-Surface Properties. *PLoS One* **10**: e0124971.

Peltier, J., Shaw, H.A., Couchman, E.C., Dawson, L.F., Yu, L., Choudhary, J.S. et al. (2015) Cyclic diGMP regulates production of sortase substrates of *Clostridium difficile* and their surface exposure through ZmpI protease-mediated cleavage. *J Biol Chem* **290**: 24453-24469.

Peniche, A.G., Savidge, T.C., and Dann, S.M. (2013) Recent insights into *Clostridium difficile* pathogenesis. *Curr Opin Infect Dis* **26**: 447-453.

Permpoonpattana, P., Hong, H.A., Phetcharaburanin, J., Huang, J.M., Cook, J., Fairweather, N.F., and Cutting, S.M. (2011) Immunization with Bacillus spores expressing toxin A peptide repeats protects against infection with *Clostridium difficile* strains producing toxins A and B. *Infect Immun* **79**: 2295-2302.

Petersohn, A., Brigulla, M., Haas, S., Hoheisel, J.D., Volker, U., and Hecker, M. (2001) Global analysis of the general stress response of *Bacillus subtilis*. *J Bacteriol* **183**: 5617-5631.

Pishdadian, K., Fimlaid, K.A., and Shen, A. (2015) SpoIIID-mediated regulation of sigmaK function during *Clostridium difficile* sporulation. *Mol Microbiol* **95**: 189-208.

Price, C.W., Fawcett, P., Ceremonie, H., Su, N., Murphy, C.K., and Youngman, P. (2001) Genome-wide analysis of the general stress response in *Bacillus subtilis*. *Mol Microbiol* **41**: 757-774.

Purcell, E.B., McKee, R.W., Bordeleau, E., Burrus, V., and Tamayo, R. (2016) Regulation of Type IV Pili Contributes to Surface Behaviors of Historical and Epidemic Strains of *Clostridium difficile*. *J Bacteriol* **198**: 565-577.

Py, B., Moreau, P.L., and Barras, F. (2011) Fe-S clusters, fragile sentinels of the cell. *Curr Opin Microbiol* **14**: 218-223.

Quereda, J.J., Pucciarelli, M.G., Botello-Morte, L., Calvo, E., Carvalho, F., Bouchier, C. et al. (2013) Occurrence of mutations impairing sigma factor B (SigB) function upon inactivation of *Listeria monocytogenes* genes encoding surface proteins. *Microbiology* **159**: 1328-1339.

Reder, A., Gerth, U., and Hecker, M. (2012a) Integration of sigmaB activity into the decision-making process of sporulation initiation in *Bacillus subtilis*. *J Bacteriol* **194**: 1065-1074.

Reder, A., Hoper, D., Gerth, U., and Hecker, M. (2012b) Contributions of individual sigmaB-dependent general stress genes to oxidative stress resistance of *Bacillus subtilis*. *J Bacteriol* **194**: 3601-3610.

Reder, A., Albrecht, D., Gerth, U., and Hecker, M. (2012c) Cross-talk between the general stress response and sporulation initiation in *Bacillus subtilis* - the sigma(B) promoter of spo0E represents an AND-gate. *Environ Microbiol* **14**: 2741-2756.

Riebe, O., Fischer, R.J., Wampler, D.A., Kurtz, D.M., Jr., and Bahl, H. (2009) Pathway for H2O2 and O2 detoxification in *Clostridium acetobutylicum*. *Microbiology* **155**: 16-24.

Rivera-Chavez, F., Zhang, L.F., Faber, F., Lopez, C.A., Byndloss, M.X., Olsan, E.E. et al. (2016) Depletion of Butyrate-Producing Clostridia from the Gut Microbiota Drives an Aerobic Luminal Expansion of Salmonella. *Cell Host Microbe* **19**: 443-454.

Rocha, E.R., Tzianabos, A.O., and Smith, C.J. (2007) Thioredoxin reductase is essential for thiol/disulfide redox control and oxidative stress survival of the anaerobe *Bacteroides fragilis*. *J Bacteriol* **189**: 8015-8023.

Rogstam, A., Larsson, J.T., Kjelgaard, P., and von Wachenfeldt, C. (2007) Mechanisms of adaptation to nitrosative stress in *Bacillus subtilis*. *J Bacteriol* **189**: 3063-3071.

Rupnik, M., Wilcox, M.H., and Gerding, D.N. (2009) *Clostridium difficile* infection: new developments in epidemiology and pathogenesis. *Nat Rev Microbiol* **7**: 526-536.

Saujet, L., Monot, M., Dupuy, B., Soutourina, O., and Martin-Verstraete, I. (2011) The key sigma factor of transition phase, SigH, controls sporulation, metabolism, and virulence factor expression in *Clostridium difficile*. *J Bacteriol* **193**: 3186-3196.
Saujet, L., Pereira, F.C., Serrano, M., Soutourina, O., Monot, M., Shelyakin, P.V. et al. (2013) Genome-wide analysis of cell type-specific gene transcription during spore formation in *Clostridium difficile*. *PLoS Genet* **9**: e1003756.
Semenyuk, E.G., Poroyko, V.A., Johnston, P.F., Jones, S.E., Knight, K.L., Gerding, D.N., and Driks, A. (2015) Analysis of Bacterial Communities during *Clostridium difficile* Infection in the Mouse. *Infect Immun* **83**: 4383-4391.
Sorg, J.A., and Sonenshein, A.L. (2008) Bile salts and glycine as cogerminants for *Clostridium difficile* spores. *J Bacteriol* **190**: 2505-2512.
Sorg, J.A., and Sonenshein, A.L. (2009) Chenodeoxycholate is an inhibitor of *Clostridium difficile* spore germination. *J Bacteriol* **191**: 1115-1117.
Soutourina, O.A., Monot, M., Boudry, P., Saujet, L., Pichon, C., Sismeiro, O. et al. (2013) Genome-wide identification of regulatory RNAs in the human pathogen *Clostridium difficile*. *PLoS Genet* **9**: e1003493.
Souza, D.G., Vieira, A.T., Soares, A.C., Pinho, V., Nicoli, J.R., Vieira, L.Q., and Teixeira, M.M. (2004) The essential role of the intestinal microbiota in facilitating acute inflammatory responses. *J Immunol* **173**: 4137-4146.
Spigaglia, P., Barketi-Klai, A., Collignon, A., Mastrantonio, P., Barbanti, F., Rupnik, M. et al. (2013) Surface-layer (S-layer) of human and animal *Clostridium difficile* strains and their behaviour in adherence to epithelial cells and intestinal colonization. *J Med Microbiol* **62**: 1386-1393.
Steiner, E., Dago, A.E., Young, D.I., Heap, J.T., Minton, N.P., Hoch, J.A., and Young, M. (2011) Multiple orphan histidine kinases interact directly with Spo0A to control the initiation of endospore formation in *Clostridium acetobutylicum*. *Mol Microbiol* **80**: 641-654.
Theriot, C.M., Koenigsknecht, M.J., Carlson, P.E., Jr., Hatton, G.E., Nelson, A.M., Li, B. et al. (2014) Antibiotic-induced shifts in the mouse gut microbiome and metabolome increase susceptibility to *Clostridium difficile* infection. *Nat Commun* **5**: 3114.
Tuchscherr, L., and Loffler, B. (2016) *Staphylococcus aureus* dynamically adapts global regulators and virulence factor expression in the course from acute to chronic infection. *Curr Genet* **62**: 15-17.
Underwood, S., Guan, S., Vijayasubhash, V., Baines, S.D., Graham, L., Lewis, R.J. et al. (2009) Characterization of the sporulation initiation pathway of *Clostridium difficile* and its role in toxin production. *J Bacteriol* **191**: 7296-7305.
van der Veen, S., and Abee, T. (2010) Importance of SigB for *Listeria monocytogenes* static and continuous-flow biofilm formation and disinfectant resistance. *Appl Environ Microbiol* **76**: 7854-7860.
van Schaik, W., van der Voort, M., Molenaar, D., Moezelaar, R., de Vos, W.M., and Abee, T. (2007) Identification of the sigmaB regulon of *Bacillus cereus* and conservation of sigmaB-regulated genes in low-GC-content gram-positive bacteria. *J Bacteriol* **189**: 4384-4390.
Vijay, K., Brody, M.S., Fredlund, E., and Price, C.W. (2000) A PP2C phosphatase containing a PAS domain is required to convey signals of energy stress to the sigmaB transcription factor of *Bacillus subtilis*. *Mol Microbiol* **35**: 180-188.
Waligora, A.J., Barc, M.C., Bourlioux, P., Collignon, A., and Karjalainen, T. (1999) *Clostridium difficile* cell attachment is modified by environmental factors. *Appl Environ Microbiol* **65**: 4234-4238.

Walter, B.M., Rupnik, M., Hodnik, V., Anderluh, G., Dupuy, B., Paulic, N. et al. (2014) The LexA regulated genes of the *Clostridium difficile*. *BMC Microbiol* **14**: 88.
Wiegand, P.N., Nathwani, D., Wilcox, M.H., Stephens, J., Shelbaya, A., and Haider, S. (2012) Clinical and economic burden of *Clostridium difficile* infection in Europe: a systematic review of healthcare-facility-acquired infection. *J Hosp Infect* **81**: 1-14.
Wilson, K.H., Kennedy, M.J., and Fekety, F.R. (1982) Use of sodium taurocholate to enhance spore recovery on a medium selective for *Clostridium difficile. J Clin Microbiol* **15**: 443-446.
Yang, X., Kang, C.M., Brody, M.S., and Price, C.W. (1996) Opposing pairs of serine protein kinases and phosphatases transmit signals of environmental stress to activate a bacterial transcription factor. *Genes Dev* **10**: 2265-2275.
Yu, Z., Qin, W., Lin, J., Fang, S., and Qiu, J. (2015) Antibacterial mechanisms of polymyxin and bacterial resistance. *Biomed Res Int* **2015**: 679109.
Zhang, Q., Feng, Y., Deng, L., Feng, F., Wang, L., Zhou, Q., and Luo, Q. (2011) SigB plays a major role in *Listeria monocytogenes* tolerance to bile stress. *Int J Food Microbiol* **145**: 238-243.

Supplemental figure legend

Figure S1: Construction of the *sigB* mutant in both 630Δ*erm* and R20291 backgrounds.

A) Scheme of the inactivation strategy of the *sigB* gene using the ClosTron technology. Primers were designed to retarget the group II intron of pMTL0007 to insert into the *sigB* gene in sense orientation immediately after the 33rd nucleotide in its coding sequence. B) Verification of the integration of the L1.LtrB intron into the *sigB* gene in 630Δ*erm* background. PCR were realised in the *sigB* mutant (lane 1, 3 and 5) and the 630Δ*erm* strain (lane 2, 4 and 6) with two primers (IMV501-IMV454) flanking the insertion site in *CD0011* (lane 3 and 4), with one primer flanking the insertion site in *CD0011* (IMV501) and the intron primer EBSu (lane 5 and 6) and primers (RAM-F/RAM-R) for the erythromycin cassette 630Δ*erm* (lane 1 and 2). C) Verification of the integration of the L1.LtrB intron into the *sigB* gene in R20291 background. The same inactivation strategy than the 630Δ*erm* strain was used in order to construct the R20291 *sigB* mutant. PCR were realised in the *sigB* mutant (lane 1, 3 and 5) and the R20291 strain (lane 2, 4 and 6) with IMV501-IMV454 (lane 5 and 6), with IMV501 and EBSu (lane 3 and 4) and with RAM-F and RAM-R (lane 1 and 2). D) Southern Blot analysis. DNA from the *sigB* mutant (lane 1) and the 630Δ*erm* strain (lane 2) were extracted and digested with *Hind*III before hybridation with a L1.LtrB intron probe.

Figure S2: Phenotypic characterisation of the *sigB* mutant.

A) Growth curve of the wild-type strain (black circle) and the *sigB* mutant (dark grey square) grown in BHI. These data represent the mean and the standard deviations of 4 independent experiments. B) Biofilm formation of the parental strain (black), the *sigB* mutant (dark grey) and the complemented strain (light grey) in BHIS supplemented with 0.1 M of glucose in both 630Δ*erm* and R20291 genetic backgrounds. After 72 h of growth in a 24-well plate, OD_{595nm} was measured after coloration with crystal violet followed by two PBS washes. The data summarised the mean and the standard deviation of 4 and 3 independent experiments for the 630Δ*erm* and the R20291 genetic backgrounds, respectively. C) Quantification of intracellular TcdA amount by Elisa sandwich in 630Δ*erm* strain and in the *sigB* mutant. Intracellular proteins were normalised at 300 $ng{\cdot}\mu l^{-1}$ for each sample. Samples were incubated for 90 min at 37°C in plates previously coated with anti TcdA polyclonal rabbit antibody at a concentration of 2 $\mu g{\cdot}ml^{-1}$. After several washes, the plates were incubated 1 h at 37°C with diluted detection antibody (anti TcdA polyclonal chicken antibody coupled with horseradish peroxidase (HRP)) at a concentration of 0.1 $\mu g{\cdot}ml^{-1}$. 3,3',5,5'-tetramethylbenzidine (TMB) solution was added and the colour was developed in the dark. OD_{450nm} was read to quantify peroxidase activity. The histogram represents the ratio of the intracellular amount of TcdA between the *sigB* mutant and the wild-type strain. D) Germination assay of the 630Δ*erm* strain (dark grey squares) and the *sigB* mutant (light grey triangles) purified spores in BHI-S supplemented with 1% of taurocholate and 1.3 mM of glycine. A negative germination control with 630Δ*erm* spores in BHI-S without taurocholate and glycine is also represented (black diamond). Values represent the $OD_{600nm}(t)/OD_{600nm}(t_0)$ ratio and are the mean of 3 independent experiments.

Figure S3: Genes differentially expressed involved in carbon metabolism and fermentation pathways.

Figure S4: Genes differentially expressed involved in peptide and amino acid metabolism.

Figure S5: Sensitivity of the *sigB* mutant to NaCl or bile salt exposure.
Serial dilutions of the 630Δ*erm* (1), the *sigB* mutant (2) and the complemented strain (3) were spotted on BHI containing 100 mM, 250 mM or 500 mM of NaCl (A), 0.01% or 0.02% of deoxycholate (B), 2 mM or 5 mM of cholate (C) and 1 $mg{\cdot}ml^{-1}$ or 2 $mg{\cdot}ml^{-1}$ of bile (D). Plates were incubated 24 h at 37°C.

<u>Figure S6:</u> Impact of the *sigB* inactivation on NO sensitivity.

A) NO and RNS stress assays. Serial dilutions of R20291 (1), R20291 *sigB*::*erm* (2) and R20291 *sigB*::*erm* + P_B-*sigB* (3) were spotted on TY plates with different DEA/NO and SNP concentrations. Plates were then incubated 24 h at 37°C. These results are representative of 4 independent experiments. B, C and D) Growth in TY of the 630Δ*erm* strain (blue), the *sigB* mutant (red) and the complemented strain (green) in presence of 0 (B), 10 (C) or 20 µM (D) of SNP, respectively. The strains were grown at 37°C in a 24-well plate sealed by an adhesive film impermeable to O_2. OD_{600nm} was monitored using a plate-reader every hour after agitation. These data are the mean of five independent experiments. In TY medium containing 10 µM of SNP, the generation time of the *sigB* mutant was 135 min^{-1} compared to 96 min^{-1} and 111 min^{-1} for the 630Δ*erm* strain and the complemented strain, respectively. In TY containing 20 µM of SNP, the generation time of the *sigB* mutant was 203 min^{-1} compared to 113 min^{-1} and 130 min^{-1} for the 630Δ*erm* strain and the complemented strain, respectively.

<u>Figure S7:</u> Assays to test the possible involvement of σ^B in the control of thiol homeostasis.

A) Diamide sensitivity assay. The histograms represent the diameter of the growth inhibition area for the 630Δ*erm* strain (black), the *sigB* mutant (dark grey) and the complemented strain (light grey). Disk diffusion assays were performed with 10 µl of 1 M diamide. Results correspond to the mean values with the standard deviations of 4 independent experiments. B) and C) Growth of *C. difficile* in the presence of air in TY soft-agar tubes containing 0.4% agar supplemented or not with 1% cysteine. B) The histograms represent the distance of growth inhibition between the top of the agar at air interface and the edge of visible bacterial growth for the 630Δ*erm* (black), the *sigB* mutant (dark grey) and the complemented strain (light grey). The data are the mean values with standard deviations of ten and five independent experiments for TY and TY supplemented with cysteine, respectively. The P-values were 7.5 x 10^{-5} for TY experiments. C) The air tolerant assay in soft agar tubes for the 630Δ*erm* strain (1 and 3) and the *sigB* mutant (2 and 4) in TY (1 and 2) and TY containing 1% cysteine (3 and 4). The white arrows indicate the interface between bacterial growth and the zone of growth inhibition.

<u>Figure S8:</u> Vegetative cells and spores enumeration in axenic mice.

Vegetative cells (A and C) and spores (B and D) were enumerated in both faecal contents (A and B) from day 2 (D2) to day 15 (D15) post-gavage and caecal contents (C and D) after sacrifice of four mice at day 2, 7 and 15 (D2, D7, D15) post-gavage for the 630Δ*erm* strain (black) and the *sigB* mutant (green). The data represent either the vegetative cells·g faeces^{-1} (or spores·g faeces^{-1}) or the vegetative cells·ml^{-1} of caecal contents (or spores·ml^{-1} of caecal contents) for each mice and the means of bacterial load in all the mice are shown in red for both strains and each days of enumeration.

Supplemental tables

Table S1: Validation of microarrays data and of the *sigB* complementation on selected genes using qRT-PCR. CDIP229: 630Δ*erm sigB*::*erm*, CDIP547: 630Δ*erm sigB*::*erm* pRPF185-P$_{sigB}$-*sigB* (see Table S8). qRT-PCR experiments were performed on three different RNA preparations for the wild-type, the *sigB* mutant and the complemented strains. The results presented correspond to the mean of at least two independent experiments.

Table S2: Sporulation and sporulation associated genes differentially controlled by σ^B in transcriptome. A gene is considered differentially expressed between the 630Δ*erm* strain and the *sigB* mutant when the P value is < 0.05 using the statistical analysis described in *Experimental procedures*. We considered genes specifically expressed during sporulation or transcribed under the control of the 4 sporulation-specific σ factors and genes encoding proteins involved in all steps of spore formation or similar to spore-associated proteins in other spore forming firmicutes.

Table S3: Genes controlled by σ^B encoding surface associated proteins. Gene names and functions correspond to those indicated in the MaGe database Clostriscope (https://www.genoscope.cns.fr). a) A gene was considered as differentially expressed between the strain 630Δ*erm* and the *sigB* mutant when the p-value is < 0.05 using the statistical analysis described in *Experimental procedures*. b) "+" indicates proteins detected in the extracellular proteome (Cafardi et al., 2013; Hensbergen et al., 2014). Other proteins under σ^B control detected in extracellular proteome such as ABC transporters (CD2174, CD2177) or others (CD1522, CD0545) are not indicated in this table. "*" means conserved in R20291 with a high level of similarity. " #" indicates c-di-GMP riboswitch, type I (CD2830-CD0245) or type II (CD2831, CD3246, CD3513).

Table S4: Genes encoding proteins involved in cell-wall metabolism controlled by σ^B in transcriptome. A gene is considered differentially expressed between the 630Δ*erm* strain and the *sigB* mutant when the P value is < 0.05 using the statistical analysis described in *Experimental procedures*.

<u>Table S5:</u> Genes encoding proteins involved in carbon, amino acid, cofactor and nucleic acid metabolism controlled by σ^B in transcriptome.

A gene is considered differentially expressed between the 630Δ*erm* strain and the *sigB* mutant when the P value is < 0.05 using the statistical analysis described in *Experimental procedures*.

<u>Table S6:</u> The expression of genes involved in oxidative stress response in strain R20291 positively controlled σ^B. qRT-PCR experiments were performed on three different RNA preparations for the R20291 strain, the *sigB* mutant (CDIP502) and the complemented strain (CDIP505). The results presented correspond to the mean of at least two independent experiments.

<u>Table S7:</u> Genes positively controlled by σ^B with an *in silico* consensus sequence likely recognised by σ^B. Using the consensus identified for σ^B of *C. difficile* upstream of mapped TSS (Fig 8), we searched its presence *in silico* in the 300-bp region upstream the translation start site of all *C. difficile* genes with the GenoList web server (<u>http://genodb.pasteur.fr/cgi-bin/WebObjects/GenoList</u>) allowing two mismatches. The genes positively controlled by σ^B in transcriptome and containing a σ^B consensus sequence in their promoter regions are listed. The -10 and -35 boxes are indicated in blue. "*" indicates the gene member of an operon regulated by σ^B in our transcriptome experiment.

<u>Table S8:</u> Strains and plasmid used in this study.

erm is a gene encoding the erythromycine resistance cassette. *cat* is a gene encoding the chloramphenicol resistance cassette leading to resistance to chloramphenicol, Cm^R and to thiamphenicol, Tm^R.

<u>Table S9:</u> Oligonucleotides used in this study.

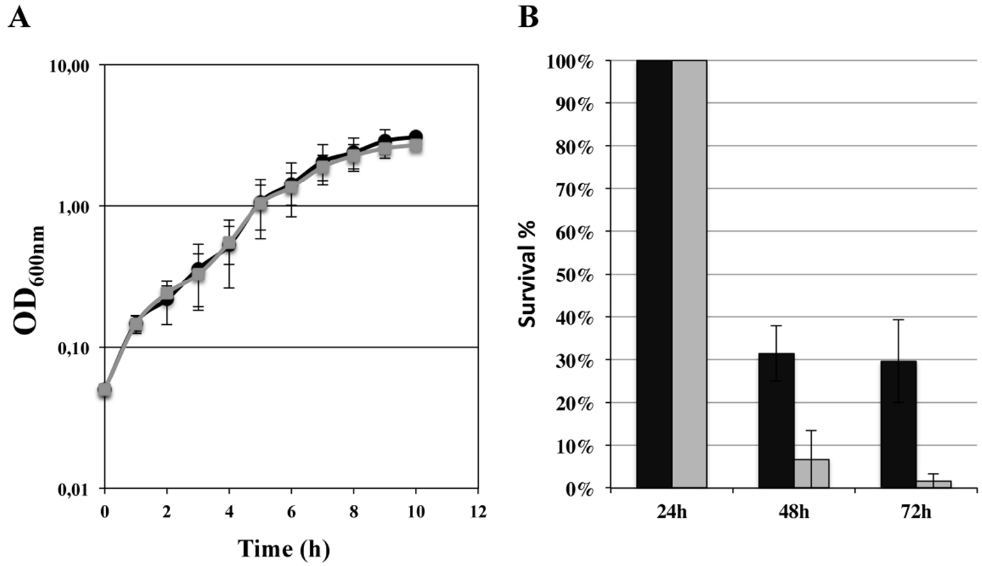

99x58mm (300 x 300 DPI)

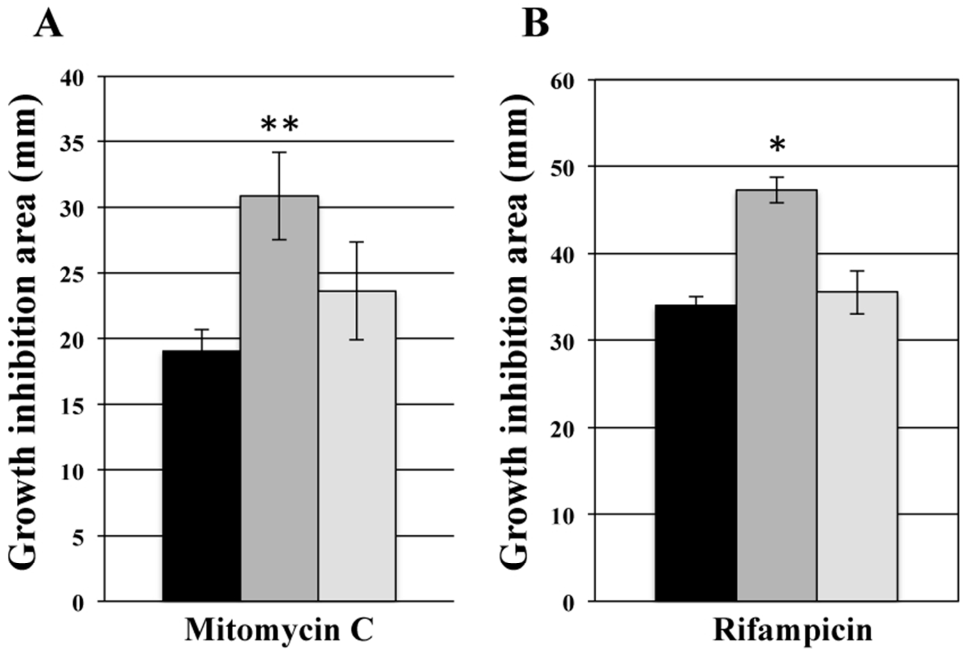

74x49mm (300 x 300 DPI)

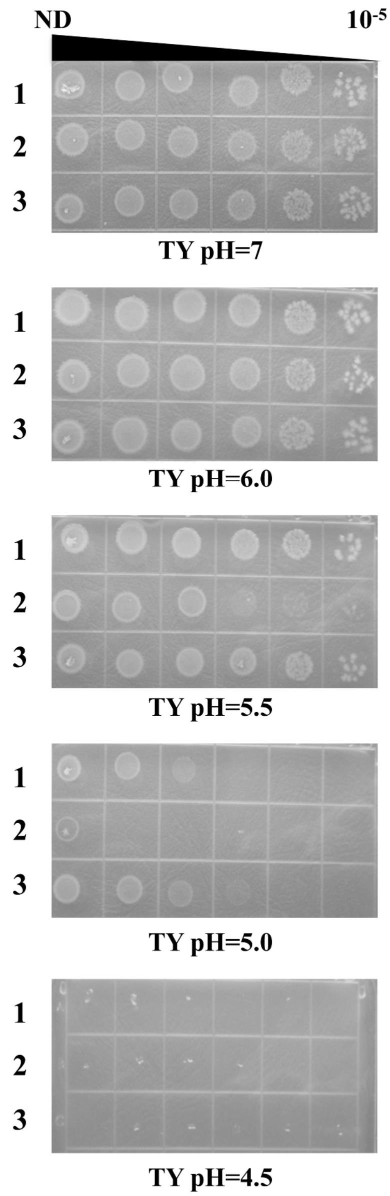

162x507mm (300 x 300 DPI)

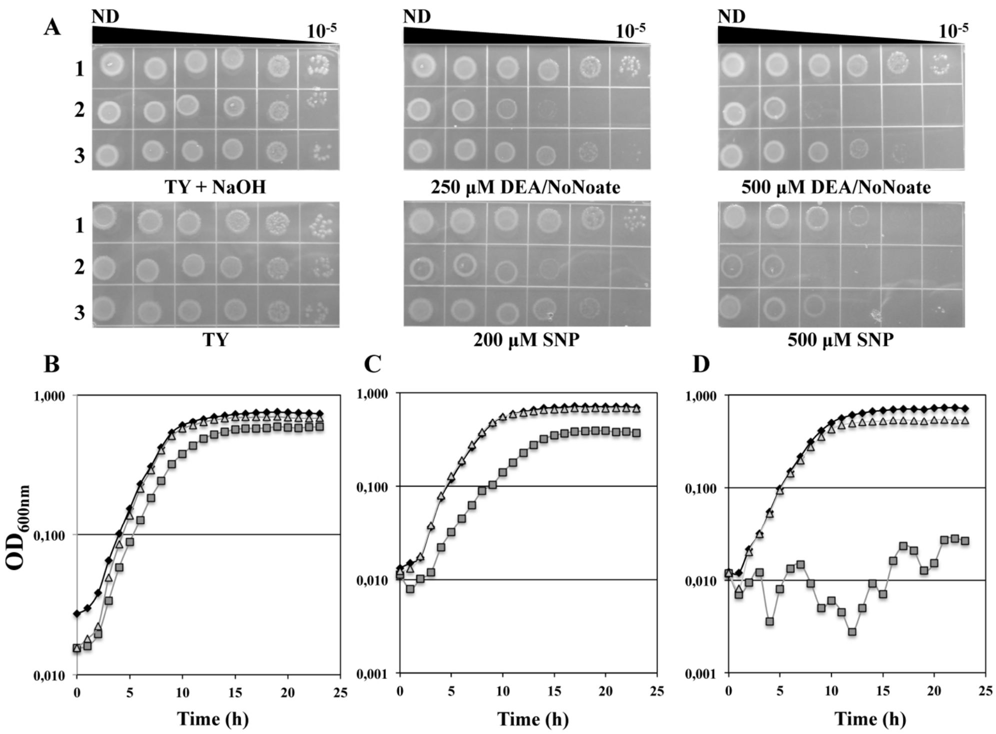

138x101mm (300 x 300 DPI)

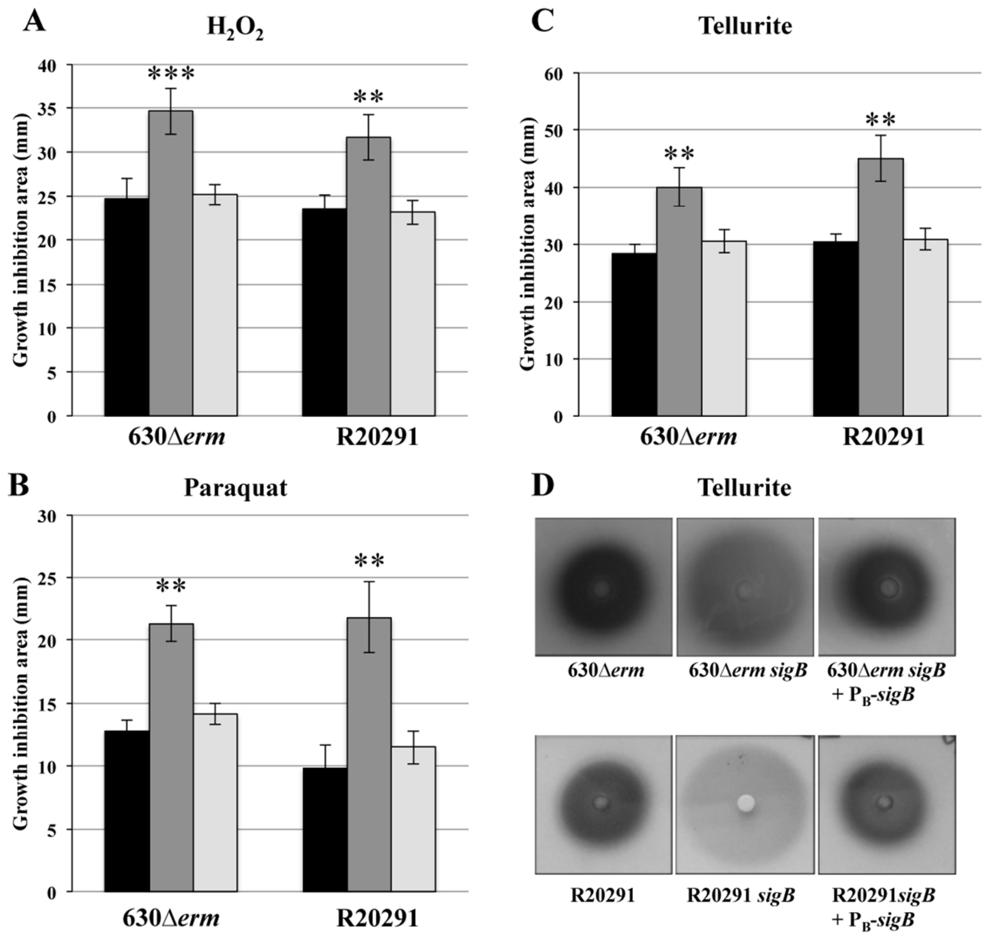

97x91mm (300 x 300 DPI)

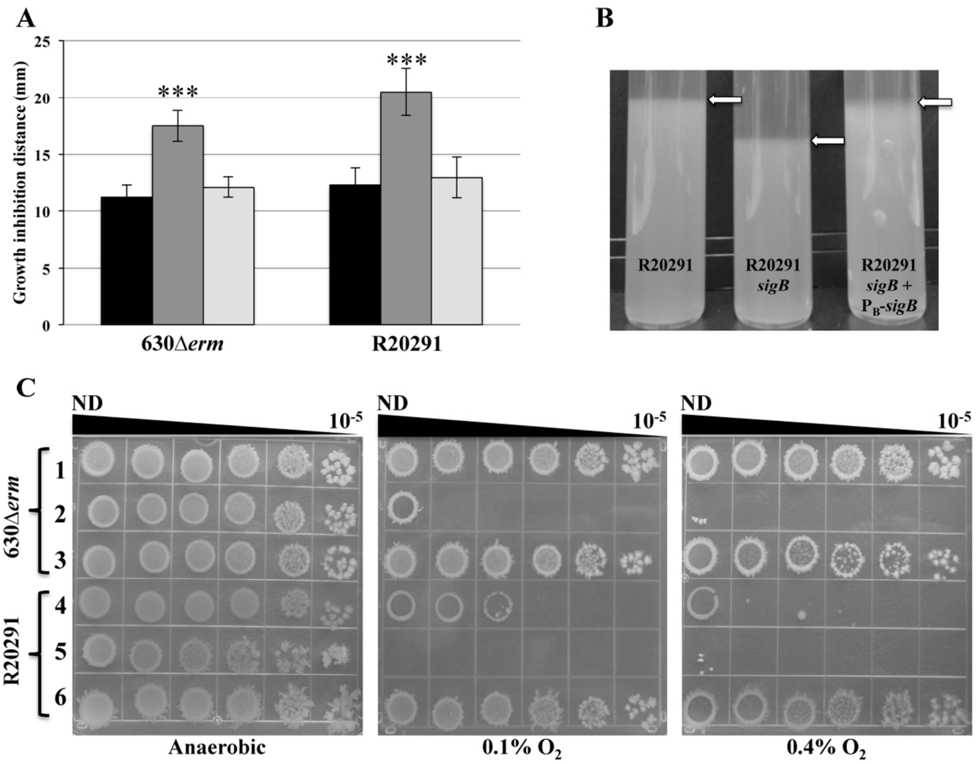

114x87mm (300 x 300 DPI)

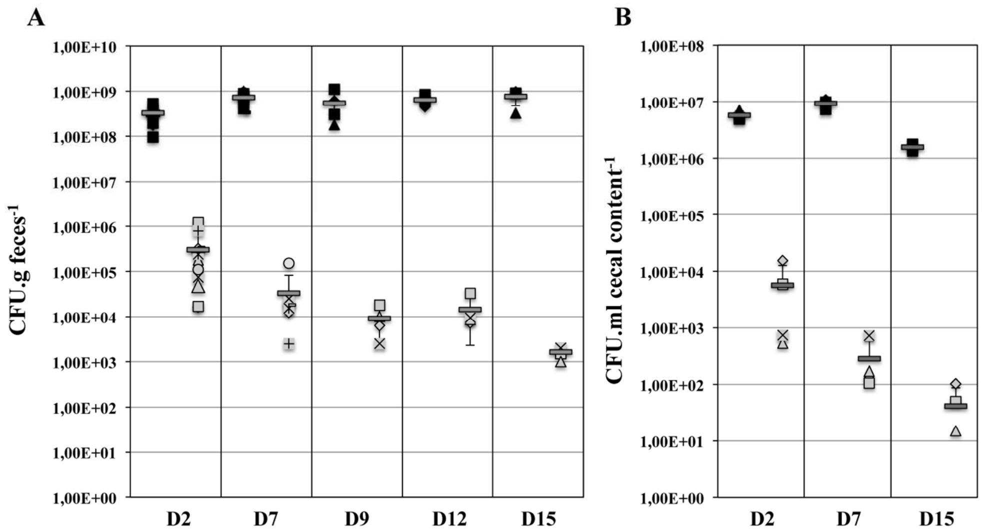

C

		D2	D7	D15
CFU.g cecal mucosa^{-1}	**630Δ*erm***	1.85×10^5	3.33×10^5	3.28×10^5
	630Δ*erm sigB*	3.79×10^1	1.05×10^1	0

132x99mm (300 x 300 DPI)

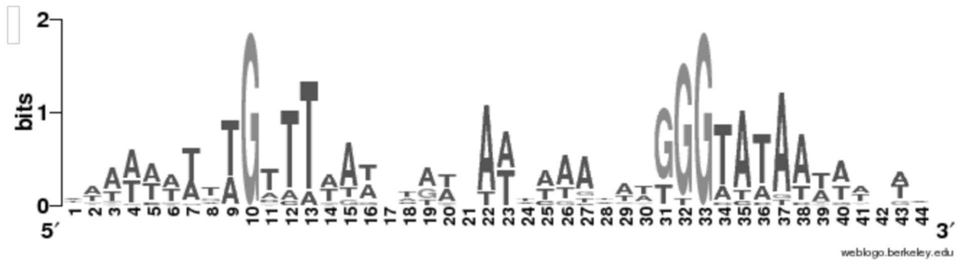

98x29mm (300 x 300 DPI)